uOttawa

A Case Study of Dissolved Oxygen Characteristics in A Wind-Induced Flow Dominated Shallow Stormwater Pond Subject to Hydrogen Sulfide Production

By

Liyu Chen

A thesis submitted under the supervision of

Dr. Robert Delatolla and Dr. Colin Rennie

In partial fulfillment of the requirements for the degree of
Masters of Applied Science in Civil Engineering

Ottawa-Carleton Institute for Civil Engineering
Department of Civil Engineering
University of Ottawa
Ottawa, Ontario, Canada

Abstract

Stormwater ponds (SWPs) are becoming increasingly important due to the negative impacts on flood mitigation and water quality control that results from rapid urbanization. These ponds are not only designed to control the discharge of large precipitation and snow melt events, but also to mitigate the water quality of the retained stormwater. Consequently, improper design and maintenance may lead to hypoxic conditions in SWPs, which result in poor water quality and generation of noxious gases. Riverside South Stormwater Pond II (RSPII) in Ottawa periodically experiences low dissolved oxygen (DO) concentrations and subsequently hypoxic conditions at depth in the pond, especially during summer days with less precipitation and winter ice covered periods. Hydrogen sulfide gas (H_2S) has been generated and released into the ambient atmosphere during these periods of lesser water quality. Hence, there is a need to understand how DO spatial distribution and seasonal change trigger and affect H_2S production. The conventional shallow design criteria of SWPs likely cause these systems to be susceptible to wind conditions. Very few research has demonstrated the correlation between wind-driven hydraulic performance and detained stormwater quality. Hence an understanding of pond-scale mixing generated by wind-induced flow and the subsequent correlation to DO concentrations and stratification in SWPs are important to understanding the water quality and performance of these systems, especially in a wind-induced flow dominated SWPs.

The overall research objective is to develop a comprehensive understanding of hypoxic conditions of SWPs and to investigate the impact of wind induced hydraulics on DO seasonal characteristics and the subsequent production of H_2S. RSPII was shown to experience lower DO and longer hypoxic conditions than an adjacent reference pond (RSPI) at both non-ice covered and ice covered months. In

addition, hypoxia was shown to be initiated at the outlet of RSPII where the depth of the pond was a maximum. Interestingly, chlorophyll-α blooms were observed during ice covered conditions in the study, with *synurids*, *tabellaria*, and *asterionella* being identified as the dominant species. A bottom-mount acoustic Doppler current profiler (aDcp) was used to collect small wind-generated currents in RSPII. The three-dimensional current and DO model produced by MIKE 3 (DHI software) suggests a conclusive result of pond scale mixing produced by wind-driven flow as well as countercurrents near the bed opposite to wind direction. A wind dominated circulation was shown to be generated even with moderate wind speed, and with a higher wind condition pond-scale complete DO mixing was created. The MIKE 3 simulation further provided a comprehensive understanding of the correlation between wind-induced hydraulics and DO concentrations distribution in a shallow stormwater pond. Therefore, this research demonstrates that wind is an essential hydraulic driver in shallow ponds, which also likely affects water quality by initiating pond mixing.

Acknowledgements

This project and subsequent thesis would not be possible without the dedication, guidance and support of so many people. A big appreciation to all the students and professors in the team and every technician in the stormwater group of the City of Ottawa. With all these efforts, the project was able to be established and accomplished. I would like to graciously thank my supervisors, Dr. Robert Delatolla and Dr. Colin Rennie, for being extremely patient, supportive and helpful. Their passion and knowledge in their specialties really inspired me during the research process. It has been a great experience working with and learning from my teammates, Patrick M. D'Aoust and Ru Wang. It needs to be mentioned that without all the help from Chris J. Melanson, Marlene Caldwell, Paul Seguin et al., stormwater technicians of the City of Ottawa, sampling during winter would be impossible. The funding provided by Natural Sciences and Engineering Research Council of Canada (NSERC) and the City of Ottawa was preeminent to the success of this project. I would also like to thank my colleges and friends who continue to be awesome and amazing. Lastly, a blowing kiss to my family that is on the other side of the earth for trusting and believing in me.

Table of Contents

List of Figures

List of Tables

List of Abbreviations

aDcp	Acoustic Doppler current profiler
BOD	Biological Oxygen Demand
COD	Chemical Oxygen Demand
Chl-α	Chlorophyll-α
DO	Dissolved Oxygen
HRT	Hydraulic retention time
H_2S	Hydrogen Sulfide
NH_3	Ammonia
NH_4^+	Ammonium
NO_3^-	Nitrate
RSPI	Riverside South Pond I
RSPII	Riverside South Pond II
SOD	Sediment Oxygen Demand
SWP	Stormwater Pond
sBOD	Soluble Biological Oxygen Demand
sCOD	Soluble Chemical Oxygen Demand
TP	Total Phosphorus

List of Symbols

σ	Constant between 0 and 1
η	Surface elevation
ω	Modified vertical velocity
ρ	Density of water
ρ_0	Reference density of water
ε	Turbulence dissipation
ε_a	Mean absolute velocity error
ε_{rms}	Root mean error
τ	Time of the day
$\sigma_k, \sigma_\varepsilon$	Empirical constant
θ_1	Arrhenius temperature coefficient for photosynthesis and respiration
θ_2	Arrhenius temperature coefficient for nitrification of ammonia to nitrite
θ_3	Arrhenius temperature coefficient for nitrification of nitrite to nitrate
θ_4	Arrhenius temperature coefficient
a	Relative day length
A	Horizontal eddy viscosity
B	Buoyancy production
$c_\mu,\ c_{1\varepsilon}, c_{2\varepsilon}, c_{3\varepsilon}$	Empirical constant
c_f	Drag coefficient
C_s	Saturation level of oxygen in water
dt	Change through time

d	Average discrepancy ratio
d	Still water depth
d_{avg}	Mean discrepancy ratio
d_{max}	Maximum discrepancy ratio
d_{min}	Minimum discrepancy ratio
f	Coriolis parameter
F_u, F_v	Horizontal stress terms
$F(N,P)$	Potential nutrient limitation
g	Gravitational acceleration
h	Total water depth
HS_BOD	Half-saturation oxygen concentration for BOD (mg O_2/L)
HS_resp	Half-saturation concentration for respiration (mg O_2/L)
HS_SOD	Half-saturation oxygen concentration for SOD (mg O_2/L)
k	Turbulent kinetic energy
K_1	Rate of reaeration
K_2	Nitrification of ammonia to nitrite rate at 20 °C (1/day)
K_3	Nitrification of nitrite to nitrate rate at 20 °C (1/day)
K_4	Degradation constant for organic matter at 20 °C (1/day)
P_a	Atmospheric pressure
P	Shear production
P_{max}	Maximum production at noon by photosynthesis
r^2	Regression coefficient of determination
R_1	Photosynthetic respiration rate at 20 °C (g O_2/m^2/day)
S	Magnitude of the discharge due to point sources

$S_{xx}, S_{xy}, S_{yx}, S_{yy}$	components of the radiation stress tensor
T	Temperature
u_S, v_S	Velocity by which the water is discharged into the ambience
U_τ	Wind shear
$U_{\tau b}$	Bed resistance
$U_{\tau s}$	Wind stress
u, v, w	Velocity components in the x, y and z direction
$\underset{u_w}{\rightarrow}$	Wind speed 10 m above the sea surface
v_t	Vertical turbulent (or eddy) viscosity
x, y, z	Cartesian coordinates
Y_1	Oxygen demand by ammonification
Y_2	Oxygen demand by nitrification
z_b	Distance from the bottom boundary condition

Chapter 1

Introduction

1.1 Problem Identification

Stormwater ponds (SWPs) and specifically retention ponds are widely used for flood and water quality control as a best management practice to mitigate the impact of runoff from highly urbanized areas (OME, 2003; Schueler, 1994). Impervious surface and altered landscapes have become the cause of reduced surface water infiltration, shorter water residence times, amplified hydrology and greater pollutant loading (Paul and Meyer, 2001; Walsh et al, 2005a,b). In addition to stormwater retention and quality enhancement, these ponds can also serve as wildlife habitat and enhance public green space (DeLorenzo et al., 2012). In areas where natural wetlands are being sacrificed to urban development, SWPs may function as breeding and foraging habitat for aquatic and terrestrial wildlife (Wren et al., 1997; Bishop et al., 2000; Sparling et al., 2004). Although SWPs are becoming an increasingly prominent and discernible component of animal and human settlements, we have little knowledge of these systems, including ecology, biochemistry and the impact of hydrology on detained water quality (Collins et al., 2010).

The City of Ottawa, Canada currently manages and maintains 108 wet SWPs, and there are as many as 1,600 stormwater facilities that are being monitored by the province of Ontario. However, if without proper design and maintenance, water quality issue may occur during the utilization of detention ponds. Following a rainfall event, contaminations settled and accumulated in sediments can be re-suspended and discharged to the environment, which may lead to less efficiency of pollution decomposition, especially for nutrients (Rad et al., 2016). The degradation of nutrients

in SWPs is dependent on the system's environmental conditions, including dissolved oxygen (DO), PH and temperature (Yates et al., 2009). Likewise, the performance of a SWP is affected by many other factors, such as hydraulic conditions, influent pollutants and vegetation, etc. (Fink and Mitsch, 2004; Kadlec, 2003). The poor performance of a stormwater pond can result in hypoxic conditions and subsequently poor water quality and the generation of noxious gases. The anaerobic reduction of sulfate is the presence of organic matter will produce hydrogen sulfide (H_2S) gas, which is a hazardous gas with unpleasant smell that may have an impact on the surrounding neighbourhood (ASCE, 1989).

Riverside South Stormwater Pond II (RSPII) in Ottawa periodically has demonstrated low DO concentrations and subsequently hypoxic conditions at depth in the pond, especially during summer droughts and winter ice covered periods. H_2S has been generated and released into the ambient atmosphere during these periods of lesser water quality. Many SWPs in Canada, and in other countries, have reported H_2S production. However, there is still a current gap of knowledge regarding H_2S generation mechanisms in these ponds and the controlling factors initiating the production of H_2S. There is thus a need to understand how the DO spatial distribution and seasonal change trigger and affect H_2S emission. To compare the DO characteristics of RSPII to a conventional pond that does not exhibit low DO conditions or H_2S production, a reference pond (RSPI) which shares similar source feed, size, and age was investigated in parallel in the study.

SWPs are commonly designed to be shallow. Andradóttir and Mortamet (2016) demonstrated wind-induced flow in a SWP with similar depths as RSPII using *in-situ* recoreded velocity measurements. Under specific weather conditions, wind was demonstrated to generate sufficient momunton to create pond-scale mixing

(Andradóttir and Mortamet, 2016). Hence, in wind-induced flow dominated SWPs, wind characteristics not only influence pond hydraulics, but also DO spatial distribution and stratification (Wium-Andersen et al., 2012). The common focus of stormwater quality studies has been evaluation of chemical and biological characteristics. Although some studies demonstrate the significance of hydraulic efficiency on SWPs with respect to pond shape, boundary configurations and topography (Jansons and Law, 2007; Glenn and Bartell, 2010; Zounemat-Kermani et al., 2015), very few of them have investigated the correlation between wind-driven hydraulic performance and detained stormwater quality.

As such, a comprehensive understanding of RSPII's unique DO conditions with consideration of wind effect on DO in the pond is essential to the design and maintenance of retention ponds in developed and developing countries.

1.2 Study objectives

The overall research objective is to develop a comprehensive understanding of hypoxic conditions of SWPs and to investigate the impact of wind induced hydraulics on DO seasonal characteristics and the subsequent production of H_2S. The goals of this study are described as follows:

1. Investigate DO conditions in both non-ice covered and ice covered seasons at two SWPs characterized by H_2S emission events (RSPII) and a reference pond (RSPI) that is adjacent to RSPII but has not demonstrated H_2S emission events;
2. Investigate the correlation of DO concentrations with chlorophyll-α (Chl-α) concentrations and biochemical oxygen demand (BOD);

3. Model three dimensional flow and DO concentrations of a wind-driven flow domain SWP (RSPII) with inclusion of chemical and biological processes;
4. Identify the impact of wind conditions on DO concentrations of a wet SWP.

These objectives were studied in two phases. The first phase was a background investigation of the seasonal bulk water concentrations of DO, Chl-α and BOD across a sampling period of approximately one year. This year of study included both non-ice covered and ice covered conditions at RSPI (a retention basin that did not have a history of H_2S emission) and RSPII (a retention basin with a history of H_2S emission). The purpose of phase one was to monitor DO seasonal characteristics and analyze its relationship with depth, spatial locations and environmental factors that include Chl-α and sBOD. Phase two focusses on the effects of pond hydraulics and in particular wind induced mixing on DO concentrations and the subsequent production of H_2S. Phase two was implemented using MIKE 3 (DHI software) with the ECOlab function of MIKE 3 hydrodynamic and water quality model.

1.3 Novel contributions

The novel contributions of this research are as follows:

- Incorporated laboratory measured bulk water quality soluble biological oxygen demand (sBOD), sediment oxygen demand (SOD), sediment nitrification kinetics, half-saturation coefficients and Arrhenius temperature coefficients in SWP 3D model;

- Implemented a new stationary acoustic Doppler current profiler (aDcp) measurement method in SWP to eliminate boat travel speed masking of in-situ velocity measurements;
- Associated wind effects to DO and H_2S production in a SWP;
- Identified high concentrations of Chl-α occurred under ice-covered SWP, likely due to the stress coping mechanism of algae.

Reference

ASCE American Society of Civil Engineers. (1989). *Sulfide in Wastewater Collection and Treatment Systems.* ASCE.

Andradóttir, H. Ó. and Mortamet, M-L. (2016). Impact of wind on storm-water pond hydraulics . *J. Hydraul. E.*

Bishop, C. A., Struger, J., Barton, D. R., Shirose, L. J., Dunn, L., Lang, A. L. and Shepherd, D. (2000). Contamination and wildlife communities in stormwater detention ponds in Guelph and the Greater Toronto Area, Ontario, 1997 and 1998. Part I-Wildlife communities. *Water Qual Res J Can*, 399-435.

Collins, K. A., Lawrence, T. J., Stander, E. K., Jontos, R. J., Kaushal, S. S., Newcomer, T. A., Grimm, N. B. and Cole Ekberg, M. L. (2010). Opportunities and challenges for managing nitrogen in urban stormwater: a review and synthesis. *Ecological Engineering*, 1507-1519.

DeLorenzo, M. E., Thompson, B., Cooper, E., Moore, J. and Fulton, M. H. (2012). A long-term monitoring study of chlorophyll, microbial contaminants, and pesticides in a coastal residential stormwater pond and its adjacent tidal creek. *Environ Monit Assess*, 343–359.

Fink, D. F. and Mitsch, W. J. (2004). Seasonal and storm event nutrient removal by a created wetland in an agricultural watershed. *Ecological Engineering*, 313-325.

Glenn, J. S. and Bartell, E. M. (2010). Evaluation short-circuiting potential of stormwater ponds. *World Environmental and Water Resources Congress*, 3942-3951.

Jansons, K. and Law, S. (2007). The hydraulic efficiency of simple stormwater ponds. *WSUD (Sydney conference)*.

Kadlec, R. H. (2003). Pond and wetland treatment . *Water Science & Technology*, 1-8.

Ontario Ministry of the Environment. (2003). *Stormwater Management Planning and Design Manual 2003*. Retrieved from Ministry of the Environment : http://www.ene.gov.on.ca/envision/gp/4329eindex.htm

Paul, M. J. and Meyer, J. L. . (2001). Streams in the urban landscape. *Annual Review of Ecology and Systematics*, 333-365.

Rad, S., Shamsudin, S., Taha, M. R. and Shahid, S. (2016). Tropical stormwater nutrient degradation using nano-TiO2 in photocatalytic reactor detention pond. *Water Science & Technology*, 405-413.

Schueler, T. (1994). The Importance of Imperviousness. *Watershed Protection Techniques*, 100-111.

Sparling, D. W., Eisemann, J. D., Kuenzel, W. (2004). Contaminant exposure and effects in red-winged blackbirds inhabiting stormwater retention ponds. *Environ Manage*, 719-729.

Walsh, C. L., Fletcher, T. D. and Ladson, A. R. . (2005a). Stream restoration in urban catchments through redesigning stormwater systems: looking to the catchment to save the stream. *Journal of the North American Benthological Society*, 690-705.

Walsh, C. L., Roy, A. H., Feminella, J. W., Cottingham, P. D., Groffman, P. M. and Morgan II, R. P. (2005b). The urban stream syndrome: current knowledge and the search for a cure. *Journal of the North American Benthological Society*, 706-723.

Wium-Andersen, T., Nielsen, A.H., Hvitved-Jacobsen, T. and Vollertsen, J. (2012). Modeling nutrient and pollutant removal in three wet detention ponds. *Urban Environment: Alliance for Global Sustainability Series*, vol. 19.

Wren, C. D., Bishop, C. A., Stewart, D. L. and Barrett, G. C. (1997). *Wildlife and contaminants in constructed wetlands and stormwater ponds: Current state of knowledge and protocols for monitoring contaminant levels and effects in wildlife.* Toronto: Canadian Wildlife Service Technical Report No. 269.

Yates, C. R. and Prasher, S. O. (2009). Phosphorus reduction from agricultural runoff in a pilot-scale surface-flow constructed wetland. *Ecological Engineering*, 1693-1701.

Zounemat-Kermani, M., Scholz, M. and Tondar, M-M. (2015). Hydrodynamic modelling of free water-surface constructed storm water wetlands using a finite volume technique. *Environmental Technology*, 2532-2547.

Chapter 2

Literature Review

2.1 Hydrological Cycle and Urban Development

The hydrological cycle describes the continuous circulation of water between the oceans, atmosphere and land (MOE, 2003). Rain and storm are the main supply of fresh water from ambient to earth through precipitation, and it returns to the atmosphere by evaporation and transpiration. Within the land phase of the hydrologic cycle, water is stored by vegetation, snowpacks, land surfaces, water bodies and subsurface soils (MOE, 2003). The renewal and regeneration of water rely on hydrological cycle (*Figure 2.1* The Hydrologic Cycle). The average annual precipitation of Ottawa, Canada from data between 1981 and 2010 was 919.48 mm (AAPCC, 2015). During wet seasons in Ottawa, precipitation can be up to 91.19 mm within a month, or even having extreme daily precipitation of 135.40 mm (Environment Canada, 2015). In Vancouver, annual precipitation between 2000 and 2006, can be as much as 1468.09 mm (Environment Canada, 2015).

Human activities are gradually changing the natural surface morphology. The surface hardening of urban areas along with the greater hydraulic efficiency of urban conveyance elements not only lead to the increased peak streamflows but also more rapid stream response (MOE, 2003). If the water cannot be absorbed by earth or be transported to other storage compartments fast enough, floods can occur during big rain events or snow melt seasons. Hence, as shown in *Figure 2.2*, the capacity of large cities to accommodate big or extreme rain events decreases dramatically due to urban development.

Moreover, human interaction and activities also have a significant influence on water quality within the hydrologic cycle. Besides generating point source pollution by extracting water for agricultural, domestic, and industrial uses, and returning as wastewater (MOE, 2003), runoff carrying numerous source of pollutants, such as nutrients, heavy metals, oil/grease and large materials coming from automobiles, lawn fertilizers, detergents etc. also act as non-point pollution which can affect nearby receiving water bodies. SWPs were introduced as not only a way for flood prevention, but also a way for water quality improvement. In terms of the removal of nutrient pollutants, many SWPs perform similarly to wastewater treatment ponds (Carleton et al., 2001). The captured runoff is detained for appropriate duration and treated through physical, chemical and biological processes within stormwater facilities (Behera and Teegavarapu, 2015). However, inappropriate pond design can generate lower treating efficiency and odours or noxious gases may be produced during the period of lesser water quality. As a result, flood control and detained water quality are two important design criteria for SWPs.

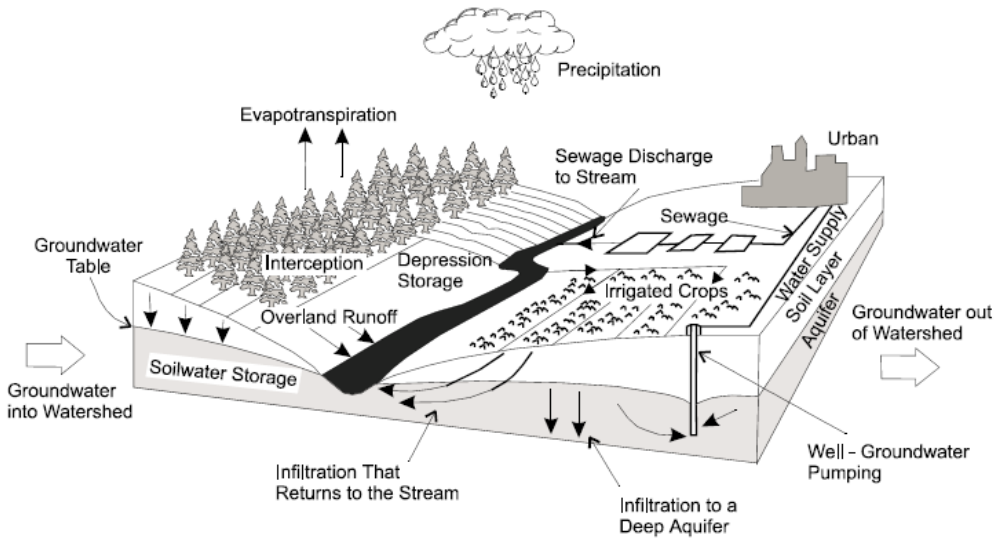

Figure 2.1 The Hydrologic Cycle (Davis M. L. and Cornwell D. A., 1991)

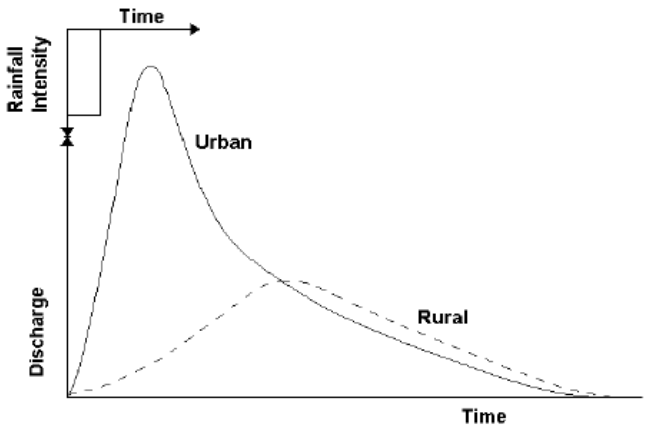

Figure 2.2 Flood Hydrographs for Urbanized and Natural Drainage Basins (Watt W. E, 1989)

2.2 Stormwater Infrastructure

A SWP can be classified as dry or wet pond according to the water level of the permanent pool. The amount of time stormwater spends in dry and wet ponds can vary between each type of pond. Dry ponds are usually built for temporary storage purpose. In storm events, dry ponds can be dual purpose facilities: detaining runoff during wet weather events; but during dry weather conditions, they provide a field area potentially suitable for a park or playground (Shammaa et al., 2002). Hence, dry ponds are more accessible towards construction and they are less susceptible to water quality issues because of the short period of retention time. Therefore, they have less impact on the surrounding environment. Wet ponds can achieve storage and purification at the same time by taking and retaining stormwater runoff. Runoff from each rain event is directed and detained in a permanent pool and treated in the pond until it is displaced by runoff from the next storm (USEPA, 1999). Usually the pond is designed to manage multiple design storms, such as 2- and/or 10-year storms, and safely pass the 100-year storm event (USEPA, 2009), and the pond basins are schemed in size of a

24 to 48 hours lag phase provison during a rain event (Olding et al., 2004). Contaminants, such as vehicle emissions and spills, oil, metals or animal feces, from urban pavement can be carried by stormwater runoff and transferred to the discharge stream or groundwater (MOE, 2003). Water purification in SWPs can be achieved by biological uptake, including algae, bacteria and vegetation uptake. In general, wet ponds can reach a better water quality management comparing to dry ponds. Drake and Guo (2008) evaluated wet ponds as preferable to the public because they create green space, wildlife habitat and are aesthetically pleasing.

A typical wet SWP, shown in *Figure 2.3*, consists of a permanent pool of water into which stormwater runoff is directed (USEPA, 1999). With respect to nonpoint source pollution control, this technology utilizes natural processes, such as wetland vegetation, solids and substrates, associated with microbial assemblages to facilitate pollutants treatment (Ouyang et al., 2011). The application of SWPs to treating degraded stream or runoff has been successfully implemented in many countries all around the world (Li et al., 2009). A forebay, as part of the permanent pool, is designed as a shallow area that is constructed for sedimentation. Sediments in SWPs increase water turbidity, inhibit plant growth and affect river biota, and likewise, contaminants that end up being adsorbed to sediments can also have deleterious impacts on receiving water bodies (Shammaa et al., 2002). Sedimentation is a common and economically friendly pre-treatment technology for settleable solids and microbes mitigation from water (Sedimentation, 2016). As runoff coming from storm sewer passes through the sediment forebay, heavier sediments get to settle down due to gravity, while lighter sediments can be resolved during the retention in the permanent pool. Shallow bathymetry and more abundant nutrients supplied from the inflow allow SWPs, especially the forebay area, to be a suitable environment for establishing

aquatic plants. Benthic flora can impede flow and trap pollutants as they enter the pond and also increase biological uptake of nutrients (USEPA, 1999).

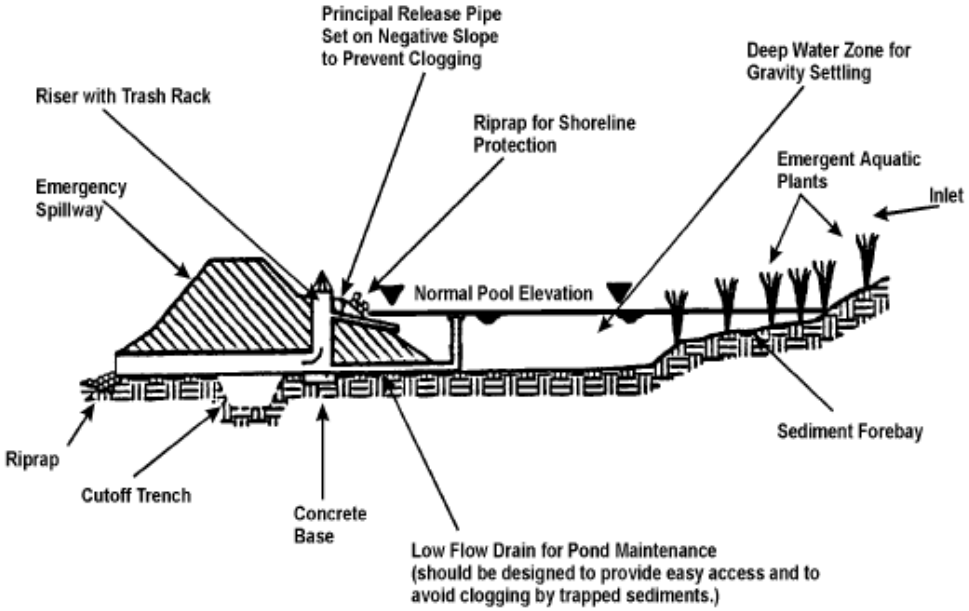

Figure 2.3 Typical layout of a wet SWP (USEPA, 1999)

2.3 SWP Water Quality

Stormwater discharges from densely populated areas using urban streams directly as receiving waters is no longer acceptable due to recreational and ecological requirements (Wagner and Geiger, 1996). One of the Best Management Practices, SWPs, allows nutrients and metals in urban runoff to settle as sediments so as to degrade and accumulate in ponds, instead of flowing directly into receiving waterbodies (McNett and Hunt, 2011). Dissolved oxygen (DO) is essential to the chemical and biological activities in SWPs. Short residence time and lack of biological activity could result in continuous passage of dissolved nutrients (NO_3^- and NH_4^+) through the pond (Mayer et al., 1996), which may lead to lower treatment efficiency. However, dissolved nutrients and organic matters degradation requires DO

consumption, which might lead to reduced water quality. Along with biological and chemical reaction of detained runoff, photosynthesis and respiration from aquatic vegetation also have an impact on the distribution of DO concentrations.

2.3.1 DO

DO is a key water quality parameter in SWPs where DO is influenced by pond bathymetry, reaeration, photosynthesis/respiration, sediment oxygen demand (SOD), soluble biochemical oxygen demand (BOD), nitrification and other nutrients (Makepeace et al., 1995). In extreme low DO conditions, which can also be defined as hypoxic conditions (DO < 2 mg/L), anaerobic bacteria utilize sulfate and organic matter present in the water system (*Figure 2.4*) to form and produce sulfide (ASCE, 1989). H_2S gas can be generated and released into the ambient atmosphere during periods of lower water quality. Meanwhile, H_2S may also have a significant negative impact on biodiversity in SWPs (Le Viol et al., 2009). Yu et al. (2012) investigated stormwater quality during dry seasons at a SWP in Korea, in which DO concentrations were reported between 7.00 to 19.00 mg/L. Likewise, Marsalek et al. (2003) and Semadeni-Davies (2006) reported that DO regimes under winter operation are related to ice cover duration in urban SWPs and the longer the isolation is, the more likely hypoxic conditions occur. Long term studies commonly focus on nutrients, microalgae or bacteria, although very few studies focus on DO seasonal characteristics of SWPs. Recently, Ku et al. (2016) demonstrated a study on H_2S emmission at a SWP in Canada. However, there is still a lack of understanding between H_2S production mechanism and DO distribution characteristics.

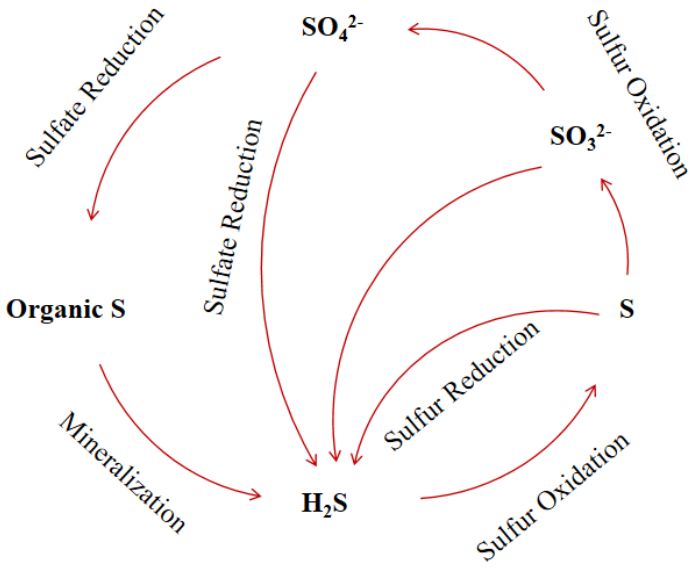

Figure 2.4 Sulfur cycle (Barton et al., 2014)

2.3.2 Chl-α

The specific load of nutrients to a wet detention pond can be significant to the development of algae (Gelbrecht et al., 2005). Chlorophyll-α (Chl-α) concentrations in the water column are used, in the study, as an indicator of the population of phytoplanktonic biomass present in the pond. Photosynthesis and respiration achieved by algae directly affects the DO concentrations (Ampe et al.,2014). Hence, Chl-α has an important relationship with DO spatial distribution and stratification in ponds. Likewise, low water circulation and overloading pollutants can cause nutrient eutrophication and harmful algal blooms, which may lead to degradation of water quality (DeLorenzo et al., 2012). Previous studies of SWPs' water quality show Chl-α concentrations ranged from 2.00 to 600.00 µg/L with higher concentrations during the summer seasons (Wium-Andersen et al., 2013; Mérette, 2012; DeLorenzo et al., 2012).

2.3.3 BOD

BOD is defined as the amount of oxygen required by bacteria to oxidize the decomposable organic matter in water sample over a certain period of time (Boyd,

1973). Chemical oxygen demand (COD) is defined as the amount of oxygen required to oxidize both organic pollutants and inorganic chemicals within water (Pisarevsky et al., 2005).

Since the BOD experimental method requires a stricter testing environment, and the COD test is more precise and quicker to execute, BOD was estimated based on measured COD concentrations in this study. A BOD/COD ratio was established and conducted for BOD concentrations estimation. Investigation shows soluble COD in SWPs range from 15.00 to 36.00 during dry seasons (Yu et al., 2012). Four levels of BOD are expected in stormwater shown in *Table 2.1*.

Table 2-1 BOD level in stormwater (Johnson et al., 2015)

BOD Level (ppm)	**Water Quality**
1 - 2	Very Good
3 - 5	Fair
6 - 9	Poor
< 100	Very Poor

2.3.4 Nitrification

Nitrification (*Figure 2.5*) is one of the main processes of the nitrogen cycle in aquatic and terrestrial systems, and is defined as the microbial oxidation of ammonium to nitrite and nitrate (Diab et al., 1993). SWP conditions, such as high DO, high PH and warm temperature can result in nitrification (Yu et al., 2012). However, the oxidation of ammonia leads to the consumption of DO through nitrification processes. Wada and Hattori (1971) and Cavari (1977) found that nitrification may be limited when the ammonium level is below 0.05-0.07 mg/L. However, on the other hand, high concentrations of free phase ammonia can also inhibit nitrification (Focht and

Verstraete, 1977). Yu et al. (2012) reported NO_3^- and NH_4^+ have a range of 0.05 to 3.00 mg/L in a stormwater wetland.

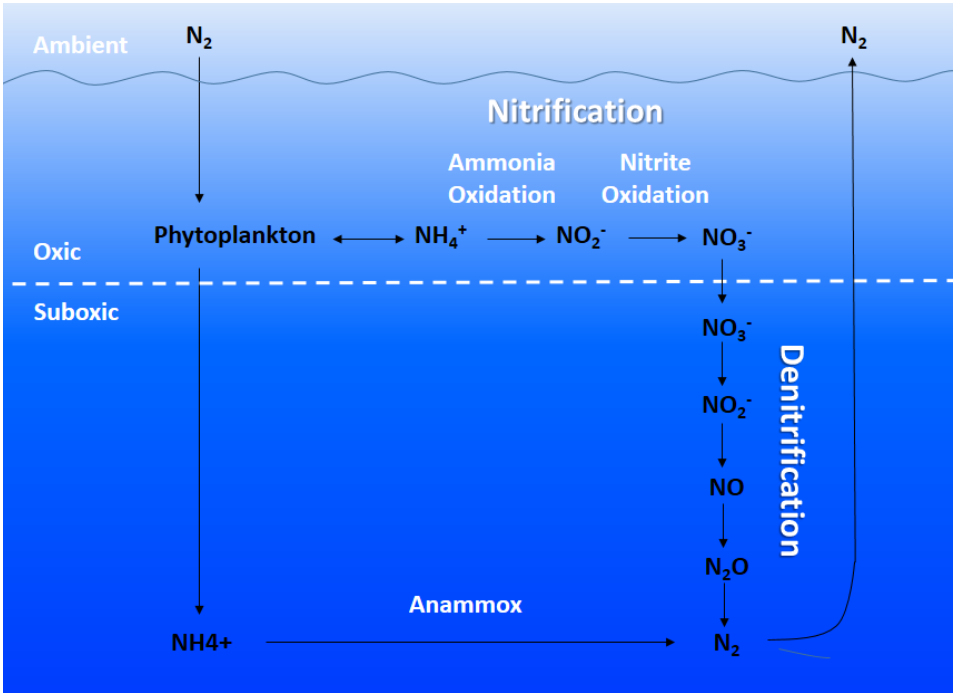

Figure 2.5 Nitrogen cycle (Gruber, 2005)

2.3.5 Phosphorus

In SWPs, phosphorus and suspended solids are often related and linked to non-point sources pollution (Yu et al., 2012). The most prevalent mode of phosphorus transport pathway (*Figure 2.6*) in SWPs is by attaching to solids and plant surface while, at the same time, being absorbed by plants, algae and microorganisms (Nairn and Mitsch, 1999; Vymazal, 2007; Yu et al., 2012). Further, phosphorus concentrations affect algae abundance so that to contribute to or consume the DO in bulk water of SWPs. The measured range of total phosphorus of 17 SWPs in Ottawa, Canada is 0.015-0.20 mg/L (Mérette, 2012).

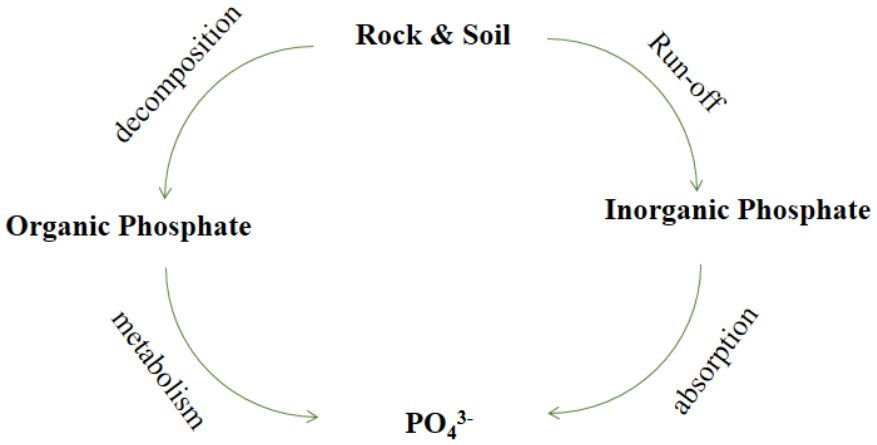

Figure 2.6 Phosphorus cycle (Paytan, A. and McLaughlin, K., 2007)

2.4 Wind impact on shallow ponds

2.4.1 Wind-induced Flow

There are mainly three control factors that result in mixing in lakes and ponds (Martin and McCutcheon, 1998): (1) the mixing energy from inflow, (2) the mixing energy from outflows or withdrawals, and (3) the transfer of energy across the air-water interface. For shallow water bodies, such as SWPs, which are known to respond to weather conditions quickly, wind-induced flow should be considered. Considerable literature presents a significant response of wind on shallow water systems in both field investigations (Kachhwal et al., 2012; Józsa, 2014) and laboratory settings (Liang et al., 2006; Pattantyus-Abraham et al., 2008; Bentzen et al., 2008; Fabian and Budinski, 2013). Fully developed countercurrent flow can be achieved, as shown in *Figure 2.7*, when no net flow over the depth is needed for mass conservation (Tsanis and Leutheusser, 1988). Momentum of the wind is partially transferred into the water column to produce waves, turbulence and large scale circulation, which can be generated even by moderate winds. The shallower the pond, the more efficient the external surface forces are induced to bottom (Józsa, 2014). Pang et al. (2015) reported

that the velocity generated by influents in Lake Taihu, China is on the order of 1.00 cm/s, while wind-produced currents can reach 5.00-10.00 cm/s.

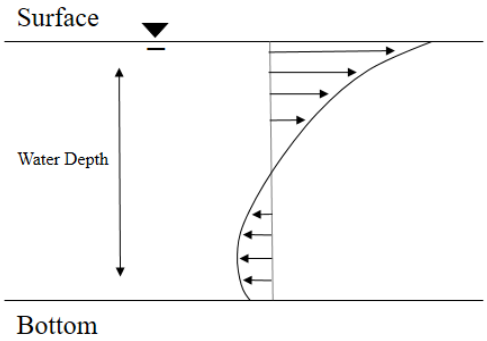

Figure 2.7 Fully developed countercurrent flow (Wu and Tsanis, 1994)

2.4.2 Pond Scale Mixing

Previous studies have demonstrated windstorms can easily generate pond-wide circulations in most shallow waters, with significant increase of flow velocities (Józsa, 2014). In fact, vorticity sources are essential to generate and maintain circulation, such as depth gradients (Simons, 1980), irregular wind field (Curto et al., 2006; Laval et al., 2003; Rueda et al., 2005) and irregular pond surface exposure to the wind (Podsetchine and Schernewski, 1999). Pond scale mixing, produced by wind, can play an important role on detained water quality in a SWP. The vast majority of stormwater quality studies have been performed in chemical and biological perspectives. Although some studies demonstrated the significance of hydraulic efficiency on SWPs with respect to pond shape, boundary configurations and topography (Jansons and Law, 2007; Glenn and Bartell, 2010; Zounemat-Kermani et al., 2015), very few of them investigate the correlation between wind-driven hydraulic performance and detained stormwater quality. Dissolved oxygen (DO) is essential to the ecological environment and treatment performance in SWPs, which can be strongly affected by waves, turbulence and large scale circulation. As such, in wind-

induced flow dominated stowmwater ponds, wind characteristics not only influence pond hydraulics, but also DO spatial distribution and stratification.

2.5 Numerical modeling of stormwater hydraulics and quality

In order to investigate wind-induced flow in a SWP and its impact on DO concentrations distribution, the two-dimensional model with average depth was not capable of simulating the changing of flow velocity and direction, as well as DO stratification along depth. Hence, a three-dimensional model, MIKE 3 (DHI software), was required. MIKE 3 flow model FM is developed for applications within oceanographic, coastal and estuarine environment, using a flexible mesh approach (MIKEbyDHI, 2012). The model is based on the numerical solution of three-dimensional incompressible Reynolds averaged Navier-Stokes equations invoking the assumptions of Boussinesq and hydrostatic pressure (MIKEbyDHI, 2012). Popular three-dimensional hydraulic modelling software includes FLOW-3D, DELFT3D, MIKE 3 etc. One common characteristic of these models is the consideration of vertical velocity components. With this, the model is able to predict vertical secondary flow and circulation pattern at cross-sections. Jin and Ji (2004), as well as Bentzen et al (2008) sucessfully simulated flow characristics variation along depth in lakes and ponds using three dimensional hydraulic software. Recently, Andradóttir and Mortamet (2016) observed wind-driven flow at a shallow SWP using velocity collection at serveral fixed locations.

Although, DO is one of the most important water quality parameters to SWPs, to the best of the authors' knowledge, no research regarding to DO conditions in a SWP have taken into consideration wind-induced pond mixing. All the chemical and biological control factors of DO concentration simulation are described in section 2.3.

Reference

American Society of Civil Engineers (ASCE). (1989). *Sulfide in Wastewater Collection and Treatment Systems.* ASCE.

Ampe, E. M., Bresciani, M., Salvadore, E., Brando, V. E., Dekker, A., Malthus, T. J., Jansen, M., Triest, L. and Batelaan, O. (2014). A wavelet approach for estimating chlorophyll-α from inland waters with reflectance spectroscopy. *IEEE Geoscience and Remote Sensing Letters*, 89-93.

Andradóttir, H. Ó. and Mortamet, M-L. (2016). Impact of wind on storm-water pond hydraulics . *J. Hydraul. E.*

AAPCC Average Annual Precipitation for Canadian Cities. (2015, 12 3). Retrieved from Current Results: http://www.currentresults.com/Weather/Canada/Cities/precipitation-annual-average.php

Barton, L. L., Fardeau, M-L. and Fauque, G. D. (2014). Hydrogen sulfide: a toxic gas produced by dissimilatory sulfate and sulfur reduction and consumed by microbial oxidation. In P. M. Kroneck, *The metal-driven biogeochemistry of gaseous compounds in the environment* (pp. 237-277). London: Springer.

Behera, P. K. and Teegavarapu, R. S. V. (2015). Optimization of a stormwater quality management pond system . *Water Resour Manage*, 1083-1095.

Bentzen, T. R., Larsen, T. and Rasmussen, M. R. (2008). Wind effects on retetion time in highway ponds. *Water Sci. Technol*, 1713-1720.

Boyd, C. E. (1973). The chemical oxygen demand of waters and biological materials from ponds. *Transactions of the American Fisheris Society* , 606-611.

Carleton, J. N., Grizzard, T. J., Godrej, A. N. and Post, H. E. (2001). Factors affecting the performance of stormwater treatment wetlands. *Water Res.*, 1552–1562.

Curto, G., Józsa, J., Napoli, E., Krámer, T. and Lipari, G. (2006). *Large scale circulations in shallow lakes.* Southampton, UK: WIT Press.

Drake, J. and Guo, Y. (2008). Maintenance of Wet Stormwater Ponds in Ontario. *Canadian Water Resources Journal* , 351-368.

DeLorenzo, M. E., Thompson, B., Cooper, E., Moore, J. and Fulton, M. H. (2012). A long-term monitoring study of chlorophyll, microbial contaminants, and pesticides in a

coastal residential stormwater pond and its adjacent tidal creek. *Environ Monit Assess*, 343–359.

Diab, S., Kochba, M. and Avnimelech, Y. (1993). Nitrification pattern in a fluctuating anaerobic-aerobic pond environment. *Wat. Rea.*, 1469-1475.

Environment Canada. (2015, 12 3). *Ottawa Average Monthly Climate Data & Extremes*. Retrieved from El Dorado Weather: http://www.eldoradocountyweather.com/canada/climate2/Ottawa.html

EPA. (1999). *Storm Water Technology Fact Sheet - Wet Detention Ponds.* Agency, United States Environmental Protection.

EPA. (2009). *Stormwater wet pond and wetland management guidebook.* Ellicott City: United States Environmental Protection Agency.

Fabian, J. and Budinski, L. (2013). Horizontal mixing in the shallow Palic Lake caused by steady and unsteady winds. *Environ. Model. Assess.*, 427-438.

Focht, D. D. and Verstraete, W. (1977). Biochemical ecology of nitrification and denitrification. *Adv. Microbiol. Ecol.* , 135-214.

Gelbrecht, J., Lengsfeld, H., Pöthig, R. and Opitz, D. (2005). Temporal and spatial variation of phosphorus input, retention and loss in a small catchment of NE Germany. *J. Hydrol*, 151-165.

Glenn, J. S. and Bartell, E. M. (2010). Evaluation short-circuiting potential of stormwater ponds. *World Environmental and Water Resources Congress*, 3942-3951.

Gruber, N. (2005). A bigger nitrogen fix. *NATURE*, 786-787.

Jansons, K. and Law, S. (2007). The hydraulic efficiency of simple stormwater ponds. *WSUD (Sydney conference)*.

Jin, K-R. and Ji, Z-G. (2004). Case Study: Modeling of Sediment Transport and Wind-Wave Impact in Lake Okeechobee. *JOURNAL OF HYDRAULIC ENGINEERING*, 1055-1067.

Józsa, J. (2014). On the internal boundary layer related wind stress curl and its role in generating shallow lake circulations. *J. Hydrol. Hydromech.*, 16-23.

Kachhwal, L. K., Yanful, E. K. and Rennie, C. D. (2012). A semi-empirical approach for estimation of bed shear stress in a tailings pond. *Environ Earth Sci*, 823-834.

Ku, J., Liang, J, Ulrich, A. and Liu, Y. (2016). Sulfide production and management in municipal stormwater retention ponds. *J. Environ. Eng.*, 04015071.

Laval, B., Imberger, J., Hodges, B.R. and Stocker, R. (2003). Modeling circulation in lakes: Spatial and temporal variations. *Limnol. Oceanogr.*, 983-994.

Le Viol, I., Mocq, J., Julliard, R., and Kerbiriou, C. (2009). The contribution of motorway stormwater retention ponds to the biodiversity of aquatic macroinvertebrates. *Biological Conservation*, 3163-3171.

Liang, Q., Borthwick, A. G. L. and Taylor, P. H. (2006). Wind-induced chaotic advection in shallow flow geometries. Part II: Non-circular basins. *J. Hydraul. Res.*, 180-188.

Li, X., Chen, M. and Anderson, B. C. (2009). Design and performance of a water quality treatment wetland in a public park in Shanghai, China. *Ecological Engineering*, 18-24.

Marsalek, P. M., Watt, W. E., Marsalek, J. and Anderson, B. C. (2003). Winter operation of an on-stream stormwater management pond. *Water Science and Technology*, 133–143.

Makepeace, D. K., Smith, D. W., and Stanley, S. J. (1995). Urban stormwater quality: Summary of contaminant data. *Critical Reviews in Environmental Science and Technology*, 93-139.

Martin, J. L. and McCutcheon, S. C. (1998). Hydrodynamic and transport for water quality modeling. *Lewis Publisher*, 355-420.

Mayer, T., Marsalek, J. and Reyes, E. D. . (1996). Nutrients and metal contaminants status of urban stormwater ponds. *Journal of Lake and Reservoir Management*, 348-363.

McNett, J. K. and Hunt, W. F. (2011). An evaluation of the toxicity of accumulated sediments in forebays of stormwater wetlands and wetponds. *Water Air Soil Pollut* , 529-538.

Mérette, M. R. (2012). *Primary production and nutrient dynamics of urban ponds.* Ottawa,Ontario, Canada: University of Ottawa, Faculty of Science.

MIKEbyDHI. (2012). *MIKE21 &MIKE3 flow model FM. Hydrodynamic and Transport Module. Scientific documentation.* Hørsholm, Denmark: DHI.

Ministry of the Environment. (2003). *Undertanding Stormwater Management: An Introduction to Stormwater Management Planning and Design.* Government of Ontario.

Nairn, R. W. and Mitsch, W. J. (1999). Phosphorus removal in created wetland ponds receiving river overflow. *Ecological Engineering*, 107-126.

Ouyang, Y., Luo, S. M. and Cui, L. H. (2011). Estimation of nitrogen dynamics in a vertical-flow constructed wetland. *Ecological Engineering*, 453-459.

Pang, C-C., Wang, F-F., Wu, S-Q. and Lai, X-J. (2015). Impact of submerged herbaceous vegetation on wind-induced current in shallow water. *Ecological Engineering*, 387-394.

Pattantyus-Abraham, M., Tel, T., Kramer, T. and Jozsa, J. (2008). Mixing properties of a shallow basin due to wind-induced chaotic flow. *Adv. Water Resour.*, 525-534.

Paytan, A. and McLaughlin, K. (2007). The oceanic phosphorus cycle. *Chemical Reviews*, 563-576.

Pisarevsky, A. M., Polozova, I. P. and Hockridge, P. M. . (2005). Chemical oxygen demand. *Russian Journal of Applied Chemistry*, 101-107.

Podsetchine, V. and Schernewski, G. (1999). The influence of spatial wind inhomogeneity on flow patterns in a small lake. *Water Research*, 3348-3356.

Rueda, F. J., Schladow, G., Monismith, S. G. and Tacey, M. T. (2005). On the effects of topography on wind and the generation of currents in a large multi-basin lake. *Hydrobiologia*, 139-151.

Sedimentation. (2016). Retrieved from Sustainable Sanitation and Water Management: http://www.sswm.info/content/sedimentation

Semadeni-Davies, A. (2006). Winter performance of an urban stormwater pond in southern Sweden. *Hydrological Processes*, 165–182.

Shammaa, Y., Zhu, D. Z., Gyurek, L. L., and Labatiuk, C. W. (2002). Effectiveness of dry ponds for stormwater total suspended solids removal. *Can. J. Civ. Eng.*, 316-324.

Simons, T. J. (1980). Circulation models of lakes and inland seas. *Canadian Bulletin of Fisheries and Aquatic Sciences*, 203.

Tsanis, I. K. and Leutheusser, H. J. (1988). The structure of turhulent shear-induced countercurrent flow. *J. Fluid Mech.*, 531-552.

Vymazal, J. (2007). Removal of nutrients in various types of constructed wetlands. *Science of the Total Environment*, 48-65.

Wada, E. and Hattori, A. . (1971). Nitrite metabolism in the euphotic layer of the central North Pacific Ocean. *Limnol. Oceanogr*, 766-772.

Wagner, A. and Geiger, W. F. (1996). New criteria for stormwater discharges into urban streams. *Wat. Dci. Tech.*, 41-48.

Wium-Andersen, T., Nielsen, A. H., Hvitved-Jacobsen, T., Brix, H., Arias, C. A. and Vollertsen, J. (2013). Modeling the eutrophication of two mature planted stormwaterponds for runoff control. *Ecological Engineering*, 601-613.

Yu, J., Park, K. and Kim, Y. (2012). Characteristics of pollutants behabior in a stormwater constructed wetland during dry days. *Front. Environ. Sci. Eng.*, 649-657.

Zounemat-Kermani, M., Scholz, M. and Tondar, M-M. (2015). Hydrodynamic modelling of free water-surface constructed storm water wetlands using a finite volume technique. *Environmental Technology*, 2532-2547.

Chapter 3

Methodology

3.1 Field Measurements

3.1.1 In-situ dissolved oxygen (DO) and temperature sampling

Measurements of DO and temperature of Riverside South Pond I (RSPI) and Riverside South Pond II (RSPII) were acquired *in-situ* using a field optical YSI ProODO DO meter (Yellow Springs, OH) during both non-ice and ice covered conditions. Various locations were chosen and recorded using Magellan ProMark3 Thales GPS unit and antenna (Santa Clara, CA). During non-ice covered months, two aluminum boats supplied by the City of Ottawa were used for navigation purpose, respectively at RSPI and RSPII. During ice covered months, sampling locations were marked on ice using objects and an ice auger was provided for coring holes to harvest DO and temperature measurements.

3.1.2 The acoustic Doppler current profiler (aDcp) and wind data collection

Velocity measurements were performed using a SonTek RIVERSURVEYOR® M9 (San Diego, CA) aDcp. The aDcp uses Doppler's principle of ultrasonic sound waves for the change in frequency of an acoustic pulse due to the relative velocities of the source and the observer (Kachhwal et al., 2012). Acoustic pulses are emitted by the aDcp unit via transducers, scatter off particles or small suspended materials present within water column, and then return to the unit as echoes. The change in frequency of the backscattered return pulse is used to calculate water velocity (Gordon, 1996). As the pulse propagates scatter occurs at locations progressively further in the water column, and corresponding backscatter is received later in time, dividing the return pulse into "range bins" allows for velocity estimation

at discrete elevations throughout the vertical profile (Kachhwal et al., 2012; Takeda, 1986). The M9 aDcp includes four 3.0 MHz beams, which are angled in a Janus arrangement at 25° from the vertical axis, which allows collection of three-dimensional velocity components. Additional description of aDcp working techniques and terminology can be found in (Simpson, 2001).

To rectify the noise that might be caused by boat movement due to the minimal velocity in RSPII, a stationary bottom-mounted system was utilized for velocity data collection in this study. *Figure 3.1 a* shows the bottom mount system used to deploy the aDcp, which was lowered and raised by rope. The instrument was controlled in real-time by hard-wire connection to a laptop in the boat (*Figure 3.1 b*). During velocity data collection, the aDcp unit was sitting at the bottom recording velocity profile from 0.45 m above the bottom and the boat was driven at least 2 m away from the collecting locations to mitigate the effect of boat movement on current velocity. In this case, the aDcp bottom tracking function was not used due to the non-identifiability of the moving ripples at the water surface. Velocity profiles were recorded for approximately 600 s at each location with vertical resolution ranging from 0.02 to 0.06 m. One challenge of bottom-mounted collection in a natural pond was vegetation. Sampling locations were carefully selected, and data were monitored in real-time, to avoid potential for macrophytes covering or disturbing the aDcp transducers.

Wind speed and direction were obtained at RSPII using a HOBOware U30 Station wind logger (Bourne, MA) and *Figure 3.1 c* shows that the wind anemometer was located at the inlet structure and securely fastened to a permanent railing at approximately 10 m above the water surface in order to minimize wind disturbances.

Figure 3.1 a) a stationary mounting system with a secured SonTek RIVERSURVEYOR M9 aDcp unit; b) in the boat collecting data; c) a mounted HOBOware U30 Station wind logger

3.1.3 Water quality and sediment samples collection

Water samples for biochemical oxygen demand (BOD), chemical oxygen demand (COD), Chlorophyll-α (Chl-α), ammonia, nitrite, nitrate, total phosphorus (TP) and total sulfide testing were collected using a Wildco 1520 C25 Kemmerer Bottle 2.2L TT water sampler (Yulee, FL). Boats were using to reach the sampling locations during non-ice covered conditions. Under ice covered period, samples were harvest physically on ice conducted by an ice anger. Due to the strict preservation requirement of sulfide, a silicone hose was added to restrict air entrainment during sample collections. Likewise, total sulfide samples were preserved with the addition of zinc acetate and sodium hydroxide solution.

Sediment samples were collected using an Ekaman dredge for laboratory kinetics testing. The dredge was disinfected with bleach solution followed by ethanol solution between each sample taking.

3.2 Constituent analyses

The water quality concentrations in this study were acquired using standard or modified standard methods: i) BOD (Modified Standard Methods 5210B), ii) COD (Hach Method 8000), iii) Chl-α (Modified Standard Methods 10200 H), iv) ammonia (Hach Method 10205), v) nitrite (Standard Methods 4500-NO^{2-}B), vi) nitrate (Standard Methods 4500-NO^{3-}B), vii) TP (Hach Method 8190) and viii) total sulfide (SM 4500-S^{2-}D). BOD and COD analyses were performed on the same sample across a total of 18 samples to establish a BOD/COD ratio. This ratio was used to convert subsequent COD measurements to BOD values to benefit from the higher accuracy of COD analytical techniques.

3.3 Numerical methods

3.3.1 Hydrodynamic modelling description

A three-dimensional hydrodynamic model MIKE 3 FM by DHI software was used to simulate the RSPII pond flow regime. Based on the small velocities inherent to RSPII, it is hypothesized that wind-driven flow may significantly contribute to the velocity profile of the pond. The model was chosen based on the capability of simulating three-dimensional flow throughout the entire water column and hence investigating the impact of wind induced flow effects. Detailed information of the hydrodynamic model can be found in MIKEbyDHI-MIKE 21 & MIKE 3 Flow Model FM Scientific Documentation (2012), and a summary of the system is provided herein. MIKE 3 flow model FM is developed for applications within oceanographic, coastal and estuarine environment, and it is based on a flexible mesh approach. A layered mesh was conducted in the study, which means unstructured mesh was used in the horizontal domain while in the vertical domain a structured mesh was obtained. The

model is based on the numerical solution of three-dimensional incompressible Reynolds averaged Navier-Stokes equations invoking the assumptions of Boussinesq and hydrostatic pressure. In this study, σ-coordinates were used for the vertical mesh, where a σ-transformation was used for velocity components. As a result, three dimensional Reynolds averaged Navier-Stokes equations are modified and expressed as follows:

$$\sigma = \frac{z - z_b}{h} \tag{1}$$

$$\frac{\partial hu}{\partial t} + \frac{\partial hu^2}{\partial x} + \frac{\partial hvu}{\partial y} + \frac{\partial h\omega u}{\partial \sigma} = fvh - gh\frac{\partial \eta}{\partial x} - \frac{h}{\rho_0}\frac{\partial P_a}{\partial x} - \frac{gh}{\rho_0}\int_z^\eta \frac{\partial \rho}{\partial x}dz - \frac{1}{\rho_0}\left(\frac{\partial S_{xx}}{\partial x} + \frac{\partial S_{xy}}{\partial y}\right) + hF_u + \frac{\partial}{\partial z}\left(\frac{v_t}{h}\frac{\partial u}{\partial \sigma}\right) + hu_S S \tag{2}$$

$$\frac{\partial hv}{\partial t} + \frac{\partial hv^2}{\partial y} + \frac{\partial huv}{\partial x} + \frac{\partial h\omega v}{\partial \sigma} = -fuh - gh\frac{\partial \eta}{\partial y} - \frac{h}{\rho_0}\frac{\partial P_a}{\partial y} - \frac{gh}{\rho_0}\int_z^\eta \frac{\partial \rho}{\partial y}dz - \frac{1}{\rho_0}\left(\frac{\partial S_{yz}}{\partial x} + \frac{\partial S_{yy}}{\partial y}\right) + hF_v + \frac{\partial}{\partial \sigma}\left(\frac{v_t}{h}\frac{\partial v}{\partial \sigma}\right) + hv_S S \tag{3}$$

$$\omega = \frac{1}{h}\left[w + u\frac{\partial d}{\partial x} + v\frac{\partial d}{\partial y} - \sigma\left(\frac{\partial h}{\partial t} + u\frac{\partial h}{\partial x} + v\frac{\partial h}{\partial y}\right)\right] \tag{4}$$

Where σ varies between 0 at the bottom and 1 at the surface; $z_b$is the distance from the bottom where the boundary condition is imposed; t is the time; x, y and z are the Cartesian coordinates; η is the surface elevation; d is the still water depth; $h = \eta + d$ represents the total water depth; u, v and w are the velocity components in the x, y and z direction, respectively; ω is the modified vertical velocity; g stands for gravitational acceleration; ρ and ρ_0 are the density of water and the reference density

of water; S_{xx}, S_{xy}, S_{yx} and S_{yy} are components of the radiation stress tensor; v_t is the vertical turbulent (or eddy) viscosity, derived from the log-law and expressed as

$$v_t = c_\mu \frac{k^2}{\varepsilon} \tag{5}$$

Where c_μ is an empirical constant and ε is the turbulence dissipation. P_a is the atmospheric pressure; u_S and v_S are the velocity by which the water is discharged into the ambient water; S the magnitude of the discharge due to point sources; F_u and F_v are the horizontal stress terms and they are described using a gradient-stress relation, which is described as

$$F_u = \frac{\partial}{\partial x}\left(2A\frac{\partial u}{\partial x}\right) + \frac{\partial}{\partial y}\left(A\left(\frac{\partial u}{\partial y} + \frac{\partial v}{\partial x}\right)\right) \tag{6}$$

$$F_v = \frac{\partial}{\partial x}\left(A\left(\frac{\partial u}{\partial y} + \frac{\partial v}{\partial x}\right)\right) + \frac{\partial}{\partial y}\left(2A\frac{\partial v}{\partial y}\right) \tag{7}$$

Where A is horizontal eddy viscosity specified using Smagorinsky formulation. f is the Coriolis parameter, which is not relevant in this study. A cell-centered finite volume method was used for spatial discretization performance. The turbulent kinetic energy and the rate of dissipation of the turbulent kinetic energy are acquired from the $k-\varepsilon$ model (Rodi, 1984).

$$\frac{\partial k}{\partial t} + \frac{\partial uk}{\partial x} + \frac{\partial vk}{\partial y} + \frac{\partial wk}{\partial z} = F_k + \frac{\partial}{\partial z}\left(\frac{v_t}{\sigma_k}\frac{\partial k}{\partial z}\right) + P + B - \varepsilon \tag{8}$$

$$\frac{\partial \varepsilon}{\partial t} + \frac{\partial u\varepsilon}{\partial x} + \frac{\partial v\varepsilon}{\partial y} + \frac{\partial w\varepsilon}{\partial z} = F_\varepsilon + \frac{\partial}{\partial z}\left(\frac{v_t}{\sigma_\varepsilon}\frac{\partial \varepsilon}{\partial z}\right) + \frac{\varepsilon}{k}(c_{1\varepsilon}P + c_{3\varepsilon}B - c_{2\varepsilon}\varepsilon) \tag{9}$$

Detail information of values of empirical constants (σ_k, σ_ε, $c_{1\varepsilon}$, $c_{2\varepsilon}$ and $c_{3\varepsilon}$) and the full description of shear production P and buoyancy production B are given in MIKEbyDHI (2012). The turbulent kinetic energy k is given by

$$k = \frac{1}{\sqrt{c_\mu}} U_\tau^2 \tag{10}$$

Where U_τ is presented as wind shear at the surface and boundary shear at the bottom. More information regarding to bed resistance $U_{\tau b}$ can be found in FredsØe (1984) and Jones et al. (2014). Wind stress $U_{\tau s}$ is developed on a drag formula (Wu, 1980; Wu and Tsanis, 1994) based on wind speed, and it is given by

$$\overline{\tau_s} = \rho_a c_d |u_w| \overline{u}_w \tag{11}$$

$$U_{\tau s} = \sqrt{\frac{\rho_a c_f |\overline{u}_w|^2}{\rho_0}} \tag{12}$$

Where $\underset{u_w}{\rightarrow}$ is the wind speed 10 m above the sea surface; c_f is a drag coefficient proposed by Wu (1980).

3.2.2 Water quality modelling description

Water quality of RSPII was modelled using MIKE 3 FM ECOlab, which is a numerical model for three-dimensional ecological modelling based on a specific hydrodynamic condition. The level 4 model conducted in this study describes processes and the physical, chemical and biological interactions between chemical and ecosystem state variables, and it is coupled to the Advection-Dispersion Modules of the DHI hydrodynamic flow models, so that transport mechanisms based on advection-dispersion can be integrated in the ECOlab simulation (MIKEbyDHI, 2016). In this study the model is used to assess the impact of wind-driven advection-dispersion on dissolved oxygen (DO) aeration, dissipation and chemical and microbial DO production and consumption mechanisms. Detail information of the water quality model can be found in MIKEbyDHI-Water Quality WQ Templates ECOlab Scientific Description (2012), and a summary of the numerical theory of DO model is described below.

Oxygen balance is described as a function of the biotic processes of photosynthesis and respiration, degradation of organic matter (decay of biological oxygen demand (BOD)), and the rate of oxygen comsuption strived by sediment (sediment oxygen demand (SOD)) and nutrient oxidation (nitrification of ammonia to nitrite and nitrite to nitrate). In equation (13), the process of ammonia to nitrite was indicated as $nitrification_1$ and nitrite to nitrate was presented as $nitrification_2$.

$$\frac{dDO}{dt} = reaeration - (Y_1 \cdot nitrification_1 + Y_2 \cdot nitrification_2) - BOD + photosynthesis \cdot F(N,P) - respiration - SOD \quad (13)$$

Where Y_1 (g O_2/g NH_4-N) is the oxygen demand by nitrification (ammonia to nitrite); Y_2 (g O_2/g NH_4-N) is the oxygen demand by nitrification (nitrite to nitrate); $F(N,P)$ is potential nutrient limitation on photosynthesis. DO processes change through time (dt). Reaeration and photosynthesis are the oxygen sources in the system. Reaeration is the process of oxygen interchange between dissolved oxygen in water and atmosphere and it occurs at the water surface in this model. Photosynthesis is described relative to a given maximum production (P_{max}) at noon, time of the day (τ) and relative day length (a). Relatively, respiration is also considered as a consumption process of oxygen. The processes of reaeration, photosynthesis and respiration are described using equations (14) to (16).

$$reaeration = K_1(C_s - DO) \quad (14)$$

$$photosynthesis = P_{max} \cdot F_1(H) \cdot \cos 2\pi\left(\frac{\tau}{a}\right) \cdot \frac{1}{dz} \quad (15)$$

$$respiration = R_1 \cdot {\theta_1}^{(T-20)} \cdot \frac{DO}{DO + HS\_resp} \cdot \frac{1}{dz} \quad (16)$$

Where K_1 is the rate of reaeration (/day), which is dependent on wind speed, flow velocity and water depth; C_s is expressed as saturation level of oxygen in water, which

varies with salinity and temperature; T is temperature; $F_1(H)$ in this case represents light dampening function, which follows the Lambert Beer Law; R_1 is photosynthetic respiration rate at 20 °C (g O_2/m^2/day) and θ_1 is the temperature coefficient for photosynthetic respiration/production; HS_resp represents half-saturation concentration for respiration; In this case, dz is the change of actual water depth from bottom to top. Due to the differentiation of light dependency along depths, oxygen production and consumption relating to photosynthesis and autotrophic respiration vary. Photosynthesis process in the model is only activated in between the period of sunrise and sunset.

Nitrification of transforming ammonia into nitrate also consumes oxygen. Detailed information regarding the nitrification process, Y_1 and Y_2 can be found in Blackburne et al. (2007). In this study, nitrification is expressed as

$$nitrification_1 = K_2 \cdot NH_3 \cdot \theta_2{}^{(T-20)} \cdot \frac{DO}{DO + HS\_nitr} \quad (17)$$

$$nitrification_2 = K_3 \cdot NO_2^- \cdot \theta_3{}^{(T-20)} \cdot \frac{DO}{DO + HS\_nitr} \quad (18)$$

Where K_2 is $nitrification_1$ rate at 20 °C (1/day); K_3 is $nitrification_2$ rate at 20 °C (1/day); θ_2 stands for temperature coefficient for $nitrification_1$ and θ_3 stands for temperature coefficient for $nitrification_2$; HS_nitr repersents half-saturation concentration for nitrification (mg O_2/L). The degradation of organic matter (BOD) is another oxygen consuming process, which is dependent on temperature, oxygen concentration and the concentration of organic materials, which can be expressed as

$$BOD = -K_4 \cdot BOD\ concentration \cdot \theta_4{}^{(T-20)} \cdot \frac{DO}{DO + HS\_BOD} \quad (19)$$

Where K_4 indicates degradation constant for organic matter at 20 °C (1/day); θ_4 is Arrhenius temperature coefficient; HS_BOD is half-saturation oxygen concentration

for BOD (mg O_2/L). SOD which occurs at the pond bed is assumed to be dependent only on oxygen concentration and temperature.

$$SOD = \frac{DO}{HS\_SOD + DO} \cdot SOD\ per\ m^2 \cdot \theta_4{}^{(T-20)} \cdot \frac{1}{dz} \quad (20)$$

Where HS_SOD is half-saturation oxygen concentration for SOD (mg O_2/L); $SOD\ per\ m^2$ is the sediment oxygen demand in unit of g/m^2/day. Finally, in the expressions above, DO, NH_3 and BOD represent the concentration of each constituent in mg/L.

Reference

Blackburne, R., Vadivelu, V. M., Yuan, Z and Keller, J. (2007). Determination of Growth Rate and Yield of Nitrifying Bacteria by Measuring Carbon Dioxide Uptake Rate. *Water Environment Research*, 2437-2445.

Chen, L. Y., Delatolla, R., Rennie, C., D'Aoust, P., Wang, R., Pick, F. and Poulain, A. A Comprehensive Study of Dissolved Oxygen Characteristics of a Stormwater Pond. *in prep.*

FredsØe, J. (1984). Turbulent boundary layers in combined wave current motion. *Hydraulic Engineering, ASCE*, 1103-1120.

Gordon, L. (1996). Acoustic Doppler current profiler-Principles of operation: A practical primer, Second ed. *RD Instruments*, 41.

Jones, O., Zyserman, J. A. and Wu, Y. (2014). In fluence of apparent roughness on pipeline design conditions under combined waves and current. *Proceedings of the ASME 2014 33rd International Conference on Ocean, Offshore and Arctic Engineering*.

Sanjou, M. and Nezu, I. (2014). Secondary current properties generated by wind-induced water waves in experiental conditions. *Advances in Oceanography and Limnology* , 1-17.

Schueler, T. (1994). The Importance of Imperviousness. *Watershed Protection Techniques*, 100-111.

SonTek. (2016). *RiverSurveyor S5/M9 SmartPulseHD Feature*. San Diego CA: SonTek Technical Note.

Takeda, Y. (1986). Velocity profile measurement by ultrasound Doppler shift method. *International journal of heat and fluid flow*, 313-318.

Chapter 4

Study of Dissolved Oxygen Characteristics of a Stormwater Pond Susceptible to Hydrogen Sulfide Emissions

4.1 Setting the context

The article presented in this chapter is entitled *A Comprehensive Study of Dissolved Oxygen Characteristics of a Stormwater Pond Susceptible to Hydrogen Sulfide Emissions* by Liyu Chen, Robert Delatolla, Alexandre Poulain, Frances Pick, Patrick D'Aoust, Ru Wang and Colin Rennie. This article presents a comprehensive understanding of dissolved oxygen (DO) spatial and seasonal characteristics of a stormwater pond (SWP) and the subsequent production of hydrogen sulfide (H_2S) in the pond. The contributions of the authors' are as follows:

Liyu Chen: Conducted literature review, performed and optimized field sampling and experiment procedure, analyzed results, and wrote the manuscript.

Robert Delatolla: Provided supervision in the development of research procedure, analysis of results, and revision of the manuscript.

Alexandre Poulain: Provided expertise, supervision and guidance.

Frances Pick: Provided expertise, supervision and guidance.

Patrick D'Aoust: Provided assistance in the collection of samples.

Ru Wang: Provided assistance in the collection of samples.

Colin Rennie: Provided supervision, analysis of results, and revision of the manuscript.

4.2 Introduction

Stormwater ponds (SWPs) were introduced as a conventional practice for flood mitigation and water quality control due to increased runoff generated from non-infiltrative urban area after precipitation events (OME, 2003; Horner et al., 2003; Klein, 1979). USEPA (2009) defines SWPs as permanent structures designed and operated to maintain aerobic conditions within the water column to prevent lesser water quality and gas generated by anaerobic activities. In addition to stormwater retention, these ponds can also serve as wildlife habitat and public green space (DeLorenzo et al., 2012).

The City of Ottawa, Ontario, Canada manages and monitors 108 wet SWPs, with greater than a thousand stormwater facilities across Canada. Hydrogen sulfide gas (H_2S) generated under anaerobic conditions has a negative impact on stormwater quality and infrastructure maintenance (ASCE, 1989). However, there is limited knowledge of dissolved oxygen (DO) seasonal characteristics in SWPs, especially during the period of H_2S gas production. As such, a fundamental study was carried out at two SWPs in Ottawa including one pond with H_2S generation and one reference pond without any water quality issue. The ponds were selected due to the similarity of size, age and drainage area, but distinct DO concentrations under specific times of operation. The problem pond experiences periodically low DO concentrations and subsequently hypoxic conditions at depth in the pond, especially across days with less precipitation in the summer and during the winter ice covered period. Moreover, H_2S was generated under hypoxic conditions and released into the ambient atmosphere during these periods of lesser water quality. Photosynthesis and respiration rendered by algae has been demonstrated to directly affect DO spatial concentrations and stratification (Ampe et al., 2014). Chlorophyll-α (Chl-α) concentrations in the water

column were used, in the study, as an indicator of the population of algae present in pond to determine an association with DO concentrations. Soluble biochemical oxygen demand (sBOD) was also monitored in this study and associated with DO concentrations.

Previous studies (Marsalek et al., 2003; Semadeni-Davies, 2006) have shown that low DO occurs in SWPs during winter operations as a result of ice cover. Very few previous studies have measured DO, Chl-α and sBOD in SWPs in both non-ice covered and ice covered conditions. Furthermore, no comparison among ponds, especially between ponds with and without H_2S production has been previously established. Hence, this study provides a fundamental understanding of DO conditions of a pond with H_2S production, including seasonal effect, spatial distribution and stratification at depths, and compares this DO distribution with a reference pond which shares similar source feed but operates without H_2S production events. Overall, the research objective is to characterize DO concentrations throughout non-ice covered (open water) and ice covered seasons and to determine correlations between DO, Chl-α and sBOD. A better understanding of the unique DO conditions of the problem pond can provide mitigation suggestions to minimize H_2S generation and to prevent this occurrence in current and future stormwater facilities.

4.3 Materials and Methods

4.3.1 Field study descriptions

Samples and *in-situ* data were obtained from two SWPs located in the same residential area of Riverside South, Ottawa. Riverside South Stormwater Pond II (RSPII) currently demonstrates H_2S production issues. The reference pond, Riverside South Stormwater Pond I (RSPI), was chosen as a reference comparison due to its

comparable geographical location, size, age, drainage area and source water, but operated without H_2S production events. Despite these similarities, RSPI was designed with shallower bathymetry conducted with shorter hydraulic retention time (HRT). RSPII is a fresh water pond constructed in an irregular shape with a surface area of approximate 45,000 m^2 (*Figure 4.1 a*). RSPII has a large forebay with maximum depth around 1.60 m, and a deep long ditch of about 2.20 m depth across the main body. The HRT of RSPII is approximately 120 days. The maximum depth of approximately 2.50 m in RSPII occurs at the outlet. The pond has undergone periodic events of H_2S since 2009 coinciding with periods of summer droughts and winter ice cover, during which reduced water quality was also demonstrated. The reference pond (RSPI) is located at the west of RSPII with a distance of 1.67 km between the two outlets. The maximum depth at the sampling location close to the RSPI outlet is slightly more than 1.50 m (*Figure 4.1 c*) and the HRT is approximately 6 days. Both RSPI and RSPII drain into a creek at the north side of the facilities, and the creek, eventually, flows into the Rideau River.

4.3.2 DO and temperature monitoring

Measurements of DO and temperature of RSPI and RSPII were acquired between July 18th, 2014 and August 25th, 2015. The sampling period included both non-ice covered open water (from July 18th to November 11th, 2014 and from March 30th, to August 25th, 2015) and ice covered conditions (from January 7th to March 20th, 2015). DO and temperature were measured in triplicate *in-situ* using a field optical YSI ProODO DO meter (Yellow Springs, OH) during both open water and ice covered conditions.

DO and temperature were recorded at RSPII at three to four specific depths where feasible (0.50 m, 1.00 m, 1.50 m and 2.00 m below the water surface or the

lower ice surface) and at various sampling locations within the pond using a Magellan ProMark3 Thales GPS unit and antenna (Santa Clara, CA) (*Figure 4.3* & *Figure 4.4*). One location in proximity to the outlet at RSPI was sampled at three specific depths (0.50 m, 1.00 m and 1.50 m below the water surface or inferior ice surface) (*Figure 4.1* Figure 4.1 a) Bathymetry of RSPII; sampling locations of Chl-α, sBOD and total sulfide at b) RSPII and c) RSPI *c*). Due to the similarity of patterns of DO and temperature being observed during non-ice covered periods in 2015, the number of sampling locations at RSPII was reduced to five at the same specific depths where feasible (*Figure 4.1 b*). Sampling frequency was also reduced from twice per week (2014) to once per week (2015) in non-ice covered conditions at both RSPI and RSPII. No spatial measurements were recorded during early winter due to the unsafe ice thickness preventing pond accessibility. In ice covered months, *in-situ* measurements were collected in quick-succession and a very specific order once the ice cap was breeched with ice-auger to avoid reaeration of the water column in the vicinity of the collected locations. DO concentrations at RSPII were subsequently interpolated using Golden Software Surfer for further analysis.

4.3.3 Water sample collection

Water samples were collected from June 6th, 2014 to August 25th, 2015 for Chl-α, sBOD, and total sulfide analysis. sBOD and total sulfide were analyzed within the whole sampling period and Chl-α analysis was initiated from October 7th, 2014 and ended on June 25th, 2015. The whole sampling period was consisted of both non-ice covered open water (from June 6th to November 11th, 2014 and from March 30th to August 25th, 2015) and ice covered conditions (from January 7th to March 20th, 2015). A Wildco 1520 C25 Kemmerer Bottle 2.2L TT water sampler (Yulee, FL) was used for water samples collection during both conditions.

Water samples were harvested at two specific depths (0.20 m and 1.50 m below the water surface or lower ice cover surface) at five locations at RSPII and one location near the outlet at RSPI (*Figure 4.1 b & c*). These were the same locations used to measure DO and temperature. To minimize the effect of oxygen entrainment on total sulfide concentrations and conclusively increase precision of total sulfide measurements, samples were immediately preserved on-site with zinc acetate and sodium hydroxide. Water samples for Chl-α analysis were collected and stored using opaque bottles to eliminate photosynthesis before lab testing. Due to the limited accessibility to the pond during early winter, water samples collection was suspended. During ice covered months, after sample holes were breached by the ice auger, water was harvested following the measurements of DO and temperature.

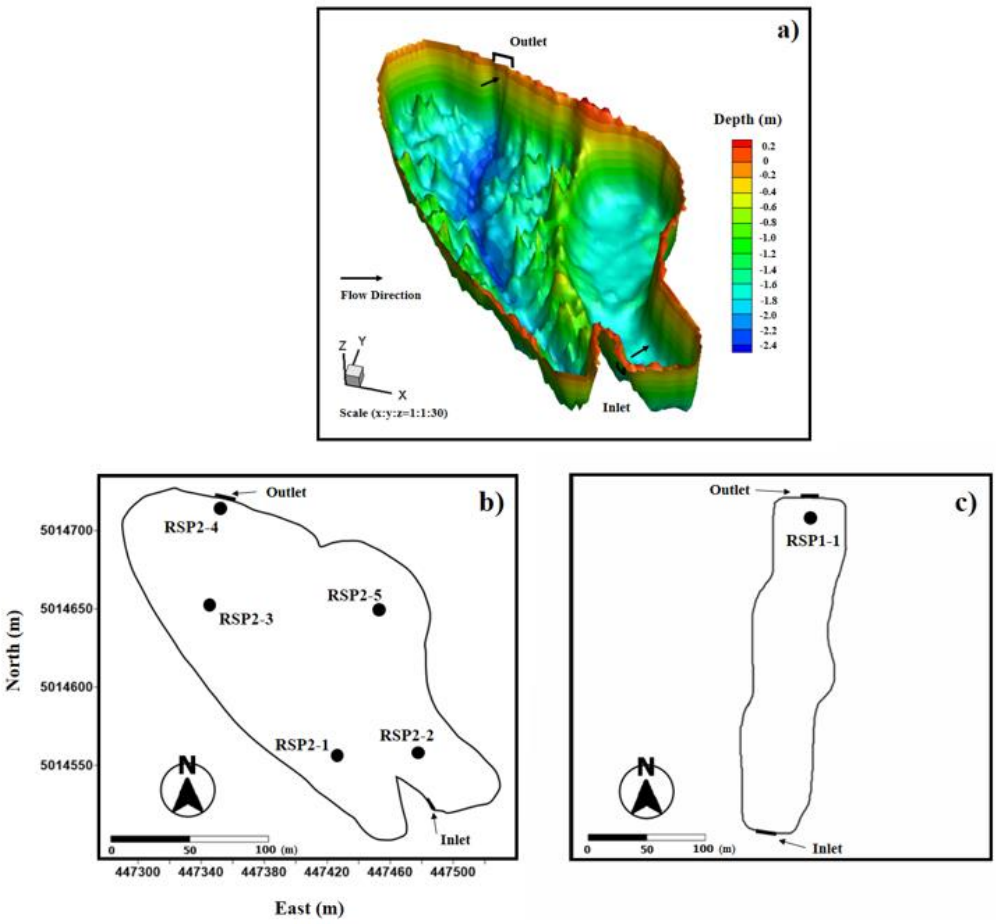

Figure 4.1 a) Bathymetry of RSPII; sampling locations of Chl-α, sBOD and total sulfide at b) RSPII and c) RSPI

4.3.4 Water quality analyses

Water samples for Chl-α analysis were filtered less than 30 hours after collection. If samples were not filtered immediately after collection, they were stored in a fridge with temperature between 0 and 4°C. 400 to 500 mL of each sample was filtered depending on the density of algae being observed and bottles were inverted several times to be homogenized before measuring the volume. A 70 mm 934-AHTM filter (glass microfiber filter) was used for filtration of each sample and the filter was folded and stored at -80 °C wrapped with aluminum sheet for light prevention. Chl-α was extracted and tested following the modified standard method 10200 H (APHA, 2012) using 95% ethanol for extraction. Visual observation of water samples on February 12th, 2015 was conducted using a phase contrast microscope for algae species identification.

Total sulfide concentrations were measured using the HACH Method 8131 (equivalent to Standard Methods 4500-S^{2-} D). sBOD to sCOD ratio was calculated for RSPII and RSPI, and used to estimate the sBOD concentrations. As the sCOD test is more precise and quicker to execute, the sBOD/sCOD ratio was quantified and used to estimate sBOD based on measured sCOD values in this study. Hach Method 8000 (APHA, 2012, equivalent to Standard Method 5220 D) was applied for sCOD analysis. sBOD/sCOD ratio was obtained 18 times during warm period with temperature range of 10 to 20 °C. An average ratio and standard deviation of 0.17 ± 0.07 was found, and an approximated sBOD/sCOD ratio of 0.20 was used for sBOD simulation in this study. This ratio was comparable to previous ratios observed in natural waters (Samudro and Mangkoedihardjo, 2010).

4.3.5 Statistical analyses

Linear regression analyses were conducted between sBOD, Chl-α and DO to evaluate the statistical significance between the data sets across the entire study. The correlation is evaluated and demonstrated using R square and *p*-values. Significance can be established with R square > 0.6 and *p*-values < 0.05.

4.4 Results and discussion

4.4.1 DO Seasonal Change at RSPII & RSPI

Figure 4.2 shows DO concentrations of four locations at RSPII (RSP2-1, RSP2-2, RSP2-3 and RSP2-4) and one location at RSPI (RSP1-1) along with the average temperatures and total sulfide concentrations at the two ponds. The DO spatial distribution maps were interpolated by kriging and plotted using Surfer® 11 by Golden Software, LLC (*Figure 4.3* & *Figure 4.4*); higher concentrations of DO being indicated as red and lower concentrations of DO indicated as purple.

During the entire measurement period encompassing both open water and ice covered conditions, DO concentrations varied from 0.4 mg/L to 16.8 mg/L at RSPII with an average concentration and 95% confidence intervals of 7.6 ± 0.4 mg/L. DO varied from 1.0 mg/L to 14.1 mg/L at RSPI with an average concentration and 95% confidence intervals of 7.9 ± 0.8 mg/L. A SWP in Kingston, Ontario, showed DO levels between 6.0 and 13.0 mg/L in non-ice covered conditions (Marsalek et al., 2003) with RSPII demonstrating a wider range of 0.6-14.9 mg/L under the same open water season of operation. The range of DO is dependent on pond size, weather conditions and numerous factors with detrimental effects on pond life being observed at DO levels below approximately 6.0 mg/L (Swistock, 2016).

Low DO at depth was experienced at RSPII during a period of approximately 16 days with an average precipitation less than 3.5 mm (between August 19th and September 3rd, 2014); where 75% of the days in time period being without recorded precipitation (*Figure 4.2 c, d & e*). Combined with a high temperature of 17.0°C and the lack of mixing within water column, these conditions resulted in hypoxic conditions at depth in the pond, which was defined as DO less than 2.0 mg/L (Hawley et al., 2006) occurring at 2.00 m depth at RSP2-4 for approximately 10 days (*Figure 4.2 b*). Although a period of 10 days of hypoxic conditions were observed at depth in RSPII in 2014, there was no significant increase in total sulfide measured during this period of low DO *(Figure 4.2 e*). A similar low DO period of 36 days was also observed in the subsequent year with 70% of the days being without recorded precipitation, with an average precipitation of 2.3 mm, and having an average temperature of 17.0°C (from June 12th to July 17th, 2015) (*Figure 4.2 c, d & e*). These conditions led to 36 days of hypoxic conditions at 2.00 m depth at RSP2-4 (*Figure 4.2 d*). A significant increase of total sulfide from approximately 40 to 630 µg/L at RSP2-4 at depth was observed during this period in 2015 (*Figure 4.2 e*). However, it should be noted that hypoxia was confined to depths at RSPII during non-ice covered seasons and that no hypoxia was report at RSPI throughout the non-ice covered operation.

Complete ice covering of RSPII was observed at the end of December, 2015 and the complete ice covered period lasted for approximately 85 days until the end of March, 2015. During ice covered conditions, which is shown as a shaded area in *Figure 4.2*, the average concentrations and 95% confidence intervals of RSPI and RSPII were 5.0 ± 1.5 mg/L and 3.0 ± 0.6 mg/L. Leppi et al. (2016) reported winter DO levels were associated with morphology, landscape position and environmental

conditions, and that the duration of ice cover appeared to negatively influence winter DO. The DO decreased from January to February, 2015 at depths of both RSPI and RSPII following the formation of complete ice covered conditions and continued to decrease during the ice covered seasons. Low DO concentrations at SWPs observed during ice covered seasons were likely due to the lack of aeration, diffusion and mixing from the surface, as well as oxygen consumption at the sediment interface due to microbial decomposition and oxidation (Muller et al., 2012). At a depth of 2.00 m at RSP2-4, hypoxic conditions persisted for a period of approximately 85 days (*Figure 4.2 d*); while at RSP1-1 at a depth of 1.50 m the hypoxic conditions endured for approximately 40 days (*Figure 4.2 c*). At all spatial locations and depths at RSPII and RSPI, DO concentrations decreased gradually one week after ice formed except for the depth of 2.00 m at RSP2-4, where hypoxia was recorded immediately after ice cover (*Figure 4.2 d*). Further, as shown in *Figure 4.2 a, b & c*, the decrease of DO concentrations occurred more rapidly at the outlet (RSP2-4) at depths of 0.50 m, 1.00 m and 1.50 m under ice covered conditions, compared to other spatial locations at RSPII and at RSPI.

Hypoxia at depth of 0.5 m below the lower surface of ice cover was observed spatially across RSPII starting from February, 2015 (approximately 30 days after complete ice cover) for an approximate period of 40 days, which likely signified a completely hypoxic bulk water column in the pond. DO concentrations at RSPI only reached a hypoxic state at a depth of 0.5 m below the lower surface of ice cover approximately 20 days after the formation of complete hypoxic conditions at RSPII and the hypoxic state only persisted at RSPI for approximately 10 days. In general, RSPII experienced a longer period of hypoxic conditions than RSPI at all depths in ice covered conditions. The production of total sulfides occurred simultaneously with

the onset of hypoxia at depth at RSPII and the smell of H_2S was reported 30 days after complete ice cover formation, which was approximately the same time when hypoxic conditions occurred within the entire water column. On the other hand, no H_2S emission was reported at RSPI during the whole ice covered period. Previous studies corroborate that it is possible to obtain DO close to zero during winter ice covered conditions in SWPs (Marsalek et al., 2003). Once fully ice cover is established the pond becomes isolated from the atmosphere, with photosynthesis, mixing and gas/heat exchange being significantly reduced (Bertilsson et al., 2013). Although investigations on SWPs in Canada (Marsalek et al., 2003) and Sweden (Semadeni-Davies, 2006) both show short periods of hypoxic conditions isolated to depths under winter operation.

During the study period, complete hypoxia throughout the water column was observed to only occur under ice cover. By comparing the DO concentrations between the surface and the bottom of RSPII, it was observed that the DO concentrations required at least 30 days to decrease across the water column. Similarly, at RSPI, a period of at least 20 days was acquired for low DO to migrate from the bottom (sampling depth of 1.5 m below the lower surface of ice cover) to the surface (sampling depth of 0.5 m below the lower surface of ice cover). DO concentrations increased following the melting of the ice cover. It took approximately 20 days for DO to increase above 2.0 mg/L at the outlet (RSP2-4) at depth.

Figure 4.4 demonstrates that with respect to the decrease of DO concentrations at RSPII throughout the entire water column and at shallow depths in proximity to the ice cover (0.50 m depth), that low DO at shallow depths was fist observed at the outlet (RSP2-4). Hypoxic conditions at shallow depths was subsequently observed to spread across the entirety of the pond as ice covered operation continued. Although low DO

was observed throughout most of the ice covered period, high concentrations of DO at RSPII were observed at 0.50 m below the lower ice surface at the beginning of January, 2015 (i.e. more than 15.00 mg/L of DO concentration was observed at shallow depths close to the ice surface on January 9th, 2015, immediately after ice cover formation (*Figure 4.4 a*). This may have been associated with higher concentrations of oxygen dissolved in low temperature water prior to ice covering. Also this local elevated DO concentration may be associated with high concentrations of Chl-α occurring in proximity to the surface during ice cover (*Figure 4.5 a*), which suggests photosynthesis may have increased DO concentrations in proximity to the surface. However, near-surface DO concentrations declined throughout the winter (*Figure 4.4*), and no significant correlations (R square: 0.01; *p*-value: 0.39) were established between DO and Chl-α, likely due to the complexity of the natural environment and the effects of other parameters on DO. As anticipated, these findings of DO investigation confirm that one of the key factors of hypoxic conditions promotion is the pond depth (Stefan et al., 1996). Besides, differences in bathymetry design, the period of ice cover and pond retention time also potentially affect hypoxic conditions in SWPs.

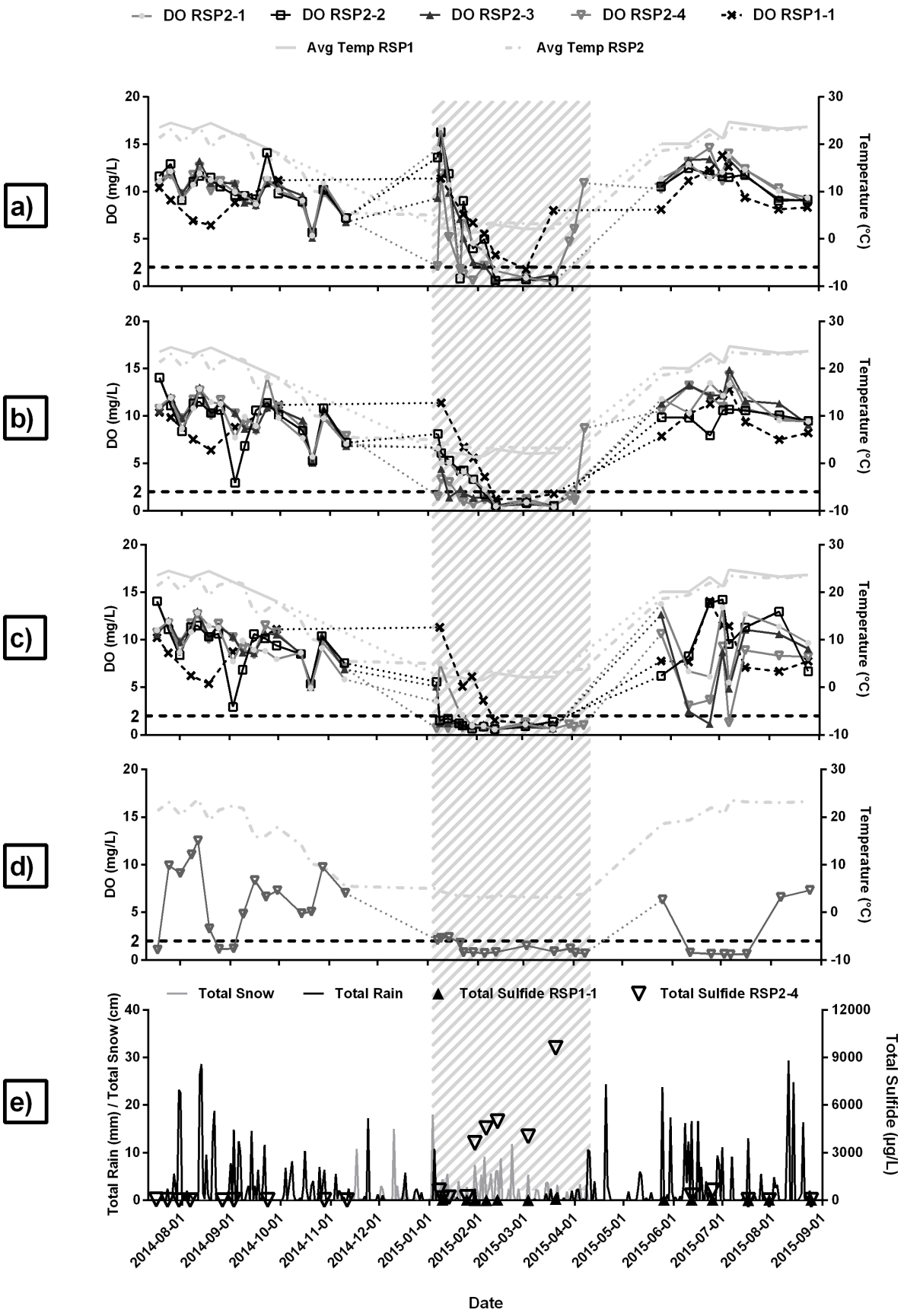

Figure 4.2 Dissolved oxygen seasonal change and averaged pond temperatures at various locations in RSPII and RSPI at depths of a) 0.50 m, b) 1.00 m, c) 1.50 m and d) 2.00 m from the water surface or the lower surface of ice cover; e) precipitation, and total sulfide concentrations at RSP2-4 & RSP1-1 at depth during the study period

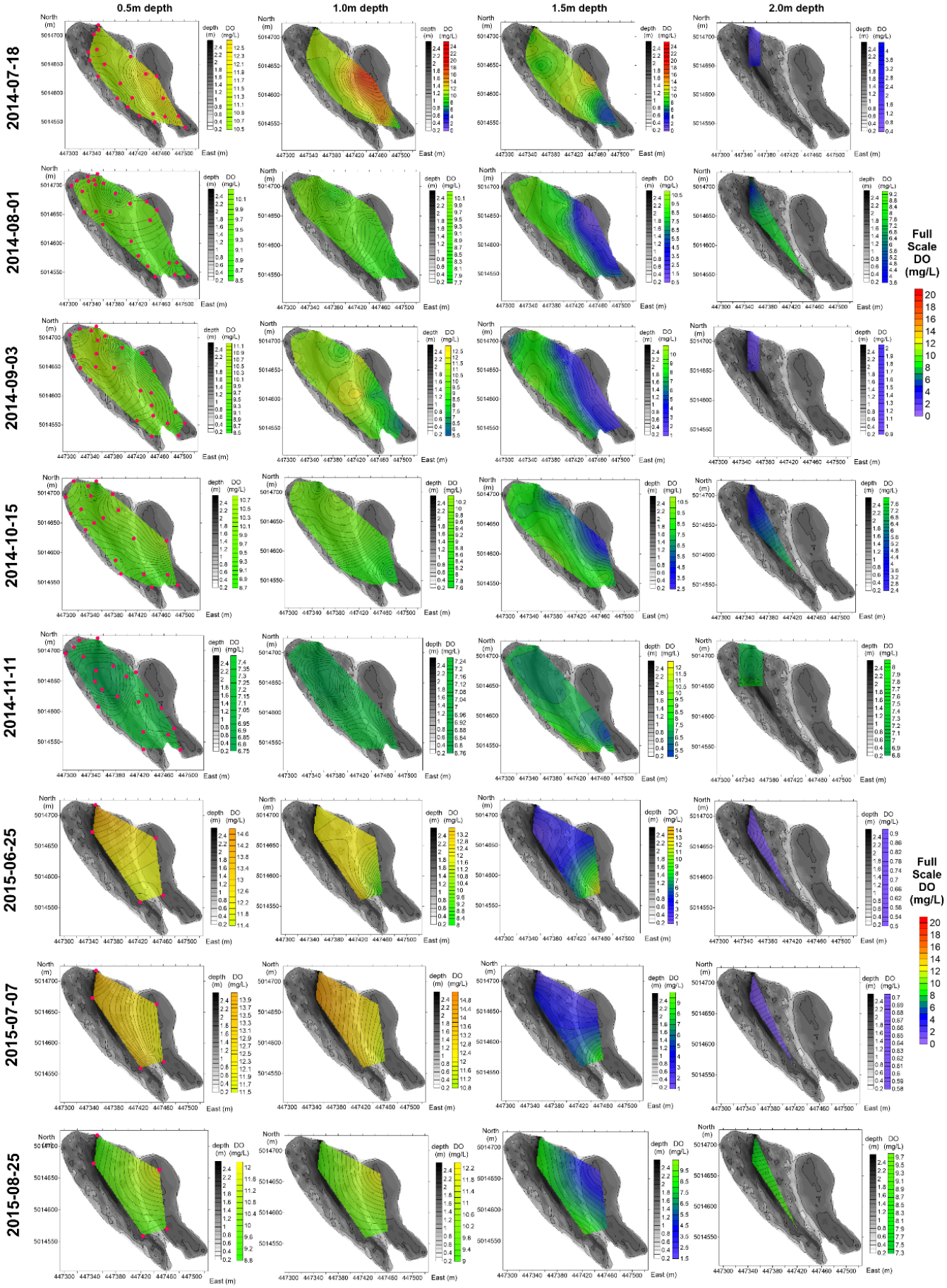

Figure 4.3 DO concentration spatial plots in RSPII at various depths of

0.50 m, 1.00 m, 1.50 m and 2.00 m with sampling locations in non-ice covered conditions

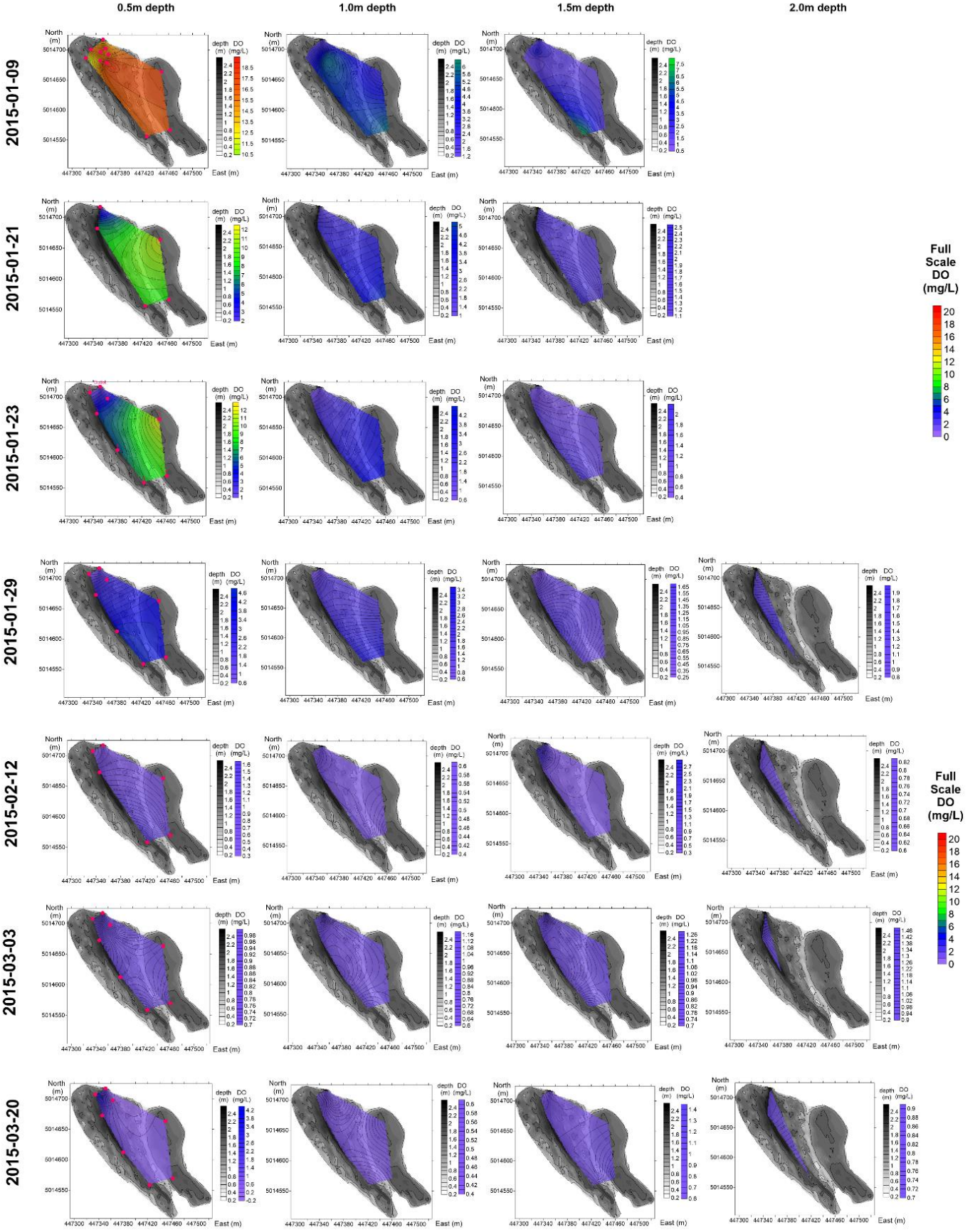

Figure 4.4 DO concentration spatial plots in RSPII at various depths of

0.50 m, 1.00 m, 1.50 m and 2.00 m with sampling locations in ice covered conditions

4.4.4 Chl-α results

An averaged concentration and 95% confidence intervals of Chl-α recorded under non-ice covered conditions at both RSPI and RSPII at both depths (0.20 m and 1.50 m below water surface) was 21.80 ± 3.34 μg/L, and the maximum concentration of 105.07 μg/L was observed at RSPII (RSP2-3) at a depth of 1.50 m below the surface (*Figure 4.5*). The Chl-α concentrations acquired in this study were within the range of 3.90 to 445.00 μg/L obtained by Mérette (2012) between June and August, 2009 from 17 SWPs in Ottawa (with an average and standard deviation of 82.66 ± 95.16 μg/L). In general, no significant difference of Chl-α concentrations at depths or locations (RSPI and RSPII), except for one anomaly (Chl-α of 105.07 μg/L at RSP2-3) was observed in non-ice covered conditions.

During ice covered conditions, comparing to ice free seasons, the average concentration and 95% confidence intervals of Chl-α decreased to 8.10 ± 1.33 μg/L at RSPI. To the contrary, the average concentration and 95% confidence intervals of Chl-α at RSPII increased to 51.29 ± 26.52 μg/L. The occurrence of Chl-α increase in winter at RSPII was likely due to the algal bloom close to the surface (at 0.20 m under the lower ice cover), according to *in-situ* observation (green water samples were observed on dates with high concentrations of Chl-α). Concentrations of Chl-α greater than 20.00-30.00 μg/L are usually considered algal bloom (Robertson et al., 2003). Even though Chl-α concentrations are generally higher in summer, there is still possibility of bloom development in winter regardless of reduced temperature and lower solar radiation (Mischke, 2014). At RSPII, high concentrations of Chl-α were observed at 0.20 m below the lower ice cover surface essentially during the whole winter of 2015 (*Figure 4.5*). The average concentration and 95% confidence intervals of Chl-α at 0.20 m below the inner ice cover at RSPII was 84.03 ± 50.01μg/L, with a

maximum concentration of 490.74 μg/L. On January 9th, 2015 the concentration of Chl-α first exceeded 150.00 μg/L at RSP2-4 and the highest concentration during ice covered conditions occurred at RSP2-5. All locations in RSPII, with the exception of RSP2-3, were observed to experience high Chl-a concentrations under ice cover conditions. *Synurids*, *tabellaria*, and *asterionella* were identified as the dominant algae taxa in the water column sample collected in RSPII on January 23rd, 2015. *Synurids* (*Figure 4.6 a & b*) are common algae mostly found in freshwater (Kristiansen, 1975) and *tabellaria (Figure 4.6 c*) along with *asterionella* (*Figure 4.6 d)* are both diatoms that are also commonly observed in fresh water bodies.

Among all the environmental factors, light is essential to algae growth (Jaud et al., 2012). Although the thickness of ice was approximately 0.5 m and was covered by several cm of snow, it was likely that some light penetrated both the snow and ice allowing algae to grow under ice covered conditions. Research on winter pond fertilization shows that despite a stressful environment, algal biomass can increase under the nutrient conditions (Mischke, 2014). RSPII showed average concentration ± 95% concentrations of nitrate of 1.02 ± 0.08 mg/L, total phosphorus of 0.24 ± 0.07 mg/L, and ammonia of 1.24 ± 0.14 mg/L. Shafi et al. (2014) found that cold stress tolerance can result in biomass increase. As such, high concentrations of Chl-α could also be understood as an escalation of algal quantity as a stress coping mechanism. In the case of algae growth in ponds, this mechanism can also increase the surface area of algae to allow more sunlight. Another explanation suggested by Larson (2000) is an increased chlorophyll to cell ratio due to the reduced light. However, research on algal bloom in winter ice covered conditions is very limited and the effect of other environmental factors cannot be neglected.

No significant correlation (R square: 0.01; *p*-value: 0.39) was found between Chl-α and DO in both non-ice covered and ice covered conditions. As shown in *Figure 4.5*, even though all the samples were collected in day time when photosynthesis pathways are active, dates with higher Chl-α concentration did not show a significant correlation with dates with higher DO. Especially during ice covered months, high Chl-α and low DO at inlet (RSP2-2) and outlet (RSP2-4) were observed at both depths (0.20 m and 1.50 m).

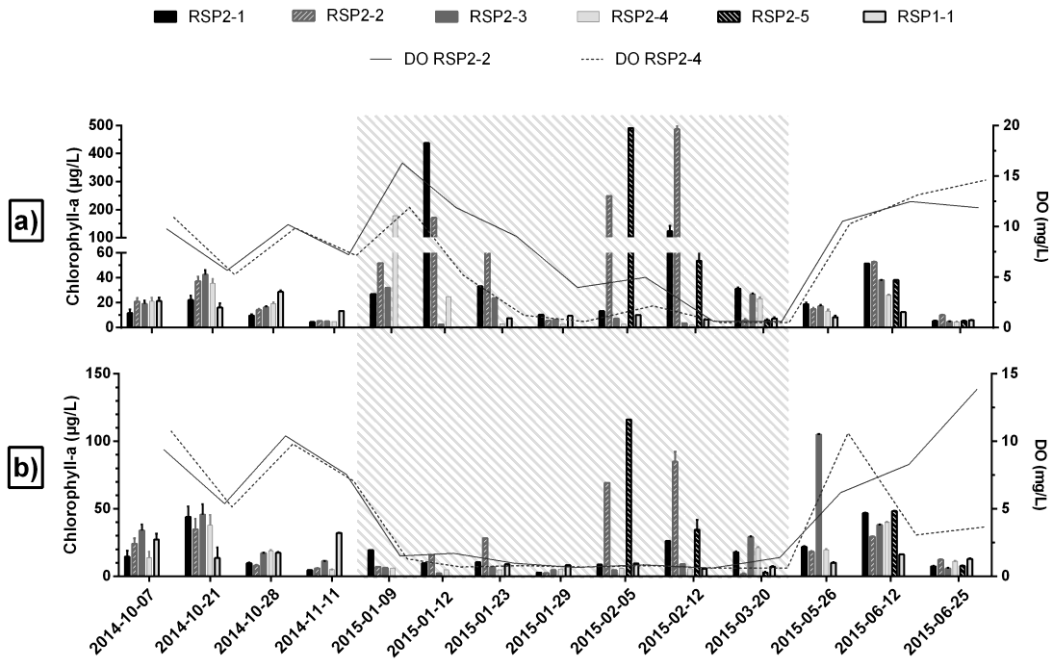

Figure 4.5 Chl-α concentration at depths of a) 0.2m and b) 1.5m from the water surface or the lower surface of ice cover in both ice-covered (shaded) and non-ice-covered conditions with dissolved oxygen concentration at RSP2-2 (inlet) and RSP2-4 (outlet)

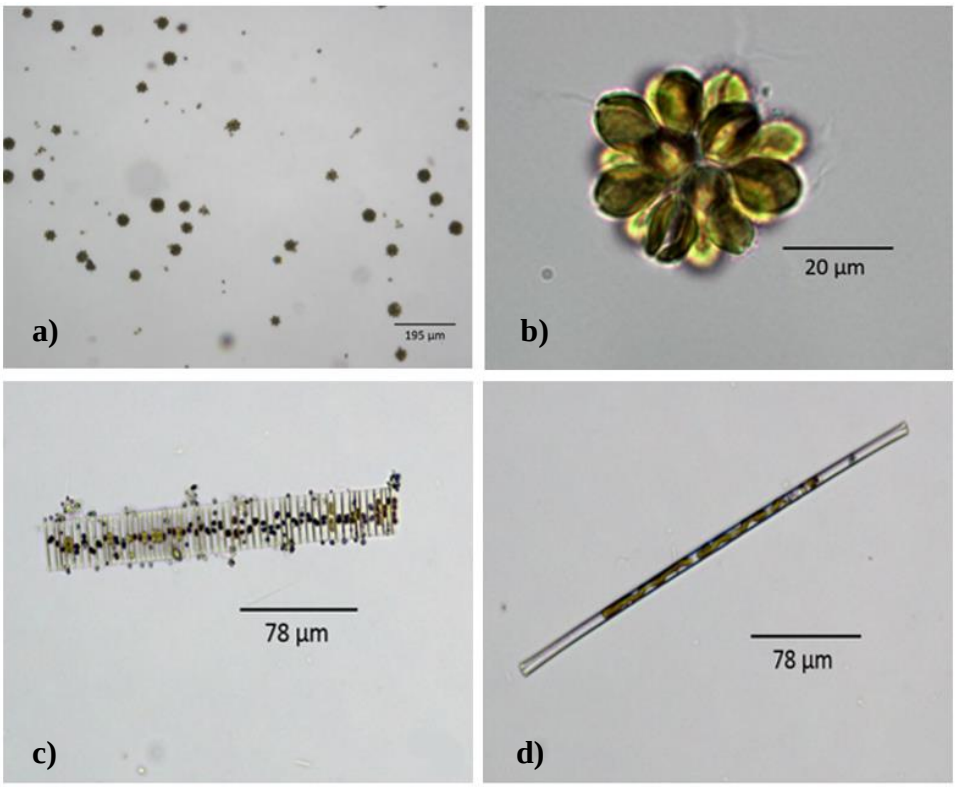

Figure 4.6 Phase contrast microscope images of a) & b) *Synurids*, c) *Tabellaria*, and d) *Asterionella* in RSPII water column

4.4.5 sBOD results

In both RSPI and RSPII, concentrations of sBOD were constant throughout the whole sampling period under ice covered and non-ice covered conditions with a small number of isolated anomalies of sBOD concentrations over 5.00 mg/L at RSPI and concentrations more than 20.00 mg/L at RSPII (*Figure 4.7 a & b*). The average concentration and 95% confidence intervals at RSPII was 3.96 ± 0.40 mg/L, which was slightly higher than the average of 3.04 ± 0.37 mg/L at RSPI. In addition, no significant difference was demonstrated between the depths of 0.20 m and 1.50 m. For shallow and low flow waterbodies, such as ponds and wetlands, organic material in water can accumulate and a high sBOD level can be expected (Johnson et al., 2015). Annual average sBOD in natural water bodies can be less than 10.00 mg/L (Abdo,

2005). With sBOD concentrations in a range of 3.00 – 5.00 mg/L, water is considered moderately clean with some organic waste, and if the concentrations exceed 10.00 mg/L, water quality is poor with large concentrations of organic matters exist (Johnson et al., 2015). The Danish Water Pollution Control Committee suggested the characteristic concentration of sBOD in urban run-off is approximately 5.00 mg/L multiplied by a factor (about 1.5-3) dependent on the return period for the design event (Hvitved-Jacobsen et al., 1994). Hence, sBOD concentrations at RSPII are in line with expectations for SWPs.

Figure 4.7 c & d shows the comparison between sBOD and DO at RSP2-2 at two specific depths (0.20 m and 1.50 m). During non-ice covered months, aerobic digestion in pond prevented higher concentrations of sBOD, and due to aeration, diffusion and photosynthesis, DO was able to be replenished into the water. In this case, lower sBOD was observed at both depths at RSP2-2 (*Figure 4.7 c & d*). In the early stage of ice covered conditions (shown as shaded area in *Figure 4.7*), spikes of both sBOD and DO at depths of 0.20 m and 1.50 m below the lower ice cover surface occurred due to cold temperature. A higher percentage of oxygen was dissolved due to the lower temperature in the first month of ice cover and sBOD likely increased due to a lag phase caused by lower metabolic kinetics of organisms consuming organic matters. sBOD and DO decreased at both depths in late winter due to aerobic digestion and the lack of new replenishing source material after a long period of ice cover with low pond inflows (*Figure 4.7 c & d*). A similar trend of sBOD and DO was also observed in RSPI across the same time period but with a lower maximum sBOD concentrations during the lag phase. Subsequently, organic material that came with the inflow after ice melt may have contributed to an increase of sBOD at the surface at RSP2-2 (*Figure 4.7 c*). However, the spatial and periodical fluctuation of

sBOD/sCOD ratio which was neglected in the study may also have had an impact on the increase and decrease of sBOD. As a result, error that was caused by the study method cannot be overlooked. The study showed no significant correlation (R square: 0.08; *p*-value: 0.66) between sBOD and DO in both non-ice covered and ice covered conditions.

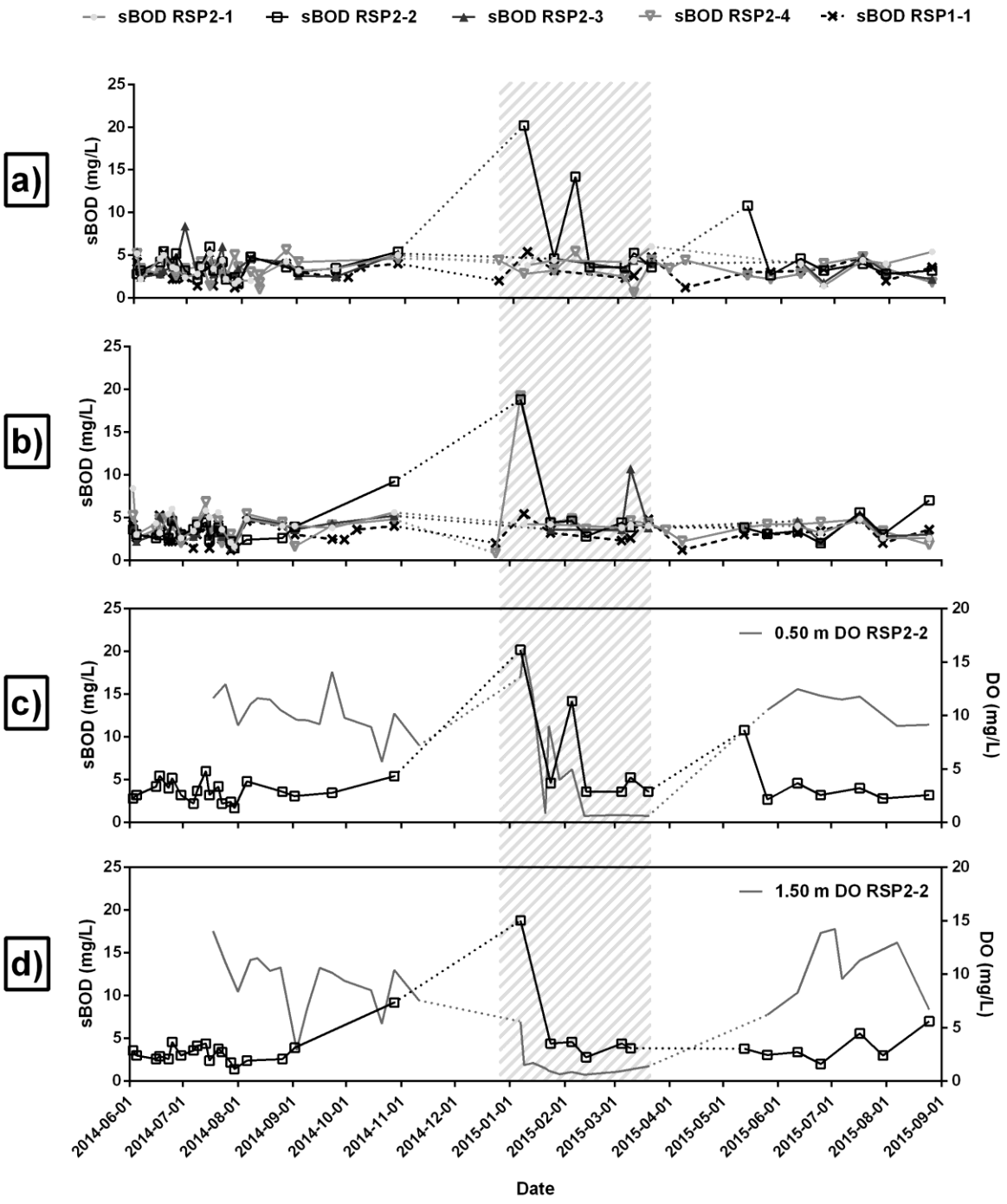

Figure 4.7 sBOD seasonal change in both non-ice and ice covered (shaded) conditions at various locations in RSPII and RSPI at depths of a) 0.20 m and b) 1.50 m from the water surface or the lower surface of ice cover; comparison of sBOD and DO at RSP2-2 (inlet) at c) 0.20 m depth (0.50 m for DO), and d) 1.50 m depth

4.4 Conclusion

The study provides a comprehensive understanding of DO seasonal characteristics at two SWPs, including one pond (RSPII) with an H_2S emission problem. Even though RSPII and RSPI show different characteristics of hypoxia (DO < 2.0 mg/L) within the same seasons, low DO tended to migrate from the bottom at both SWPs. The investigation also illustrates a significant impact of hypoxic conditions on the concentrations of total sulfide, which is related to the potential production of H_2S gas. RSPII experienced hypoxia at depth during periods with less precipitation in non-ice covered open water conditions, but no hypoxic conditions were perceived at RSPI across the same time period. During the ice free period, low DO was confined at depth, but with the hindering of reaeration under ice cover, hypoxia was able to migrate to the surface creating complete hypoxic conditions. Even though both RSPI and RSPII illustrated lower DO during ice covered conditions, pond-scale hypoxic conditions in RSPII occurred sooner and persisted for a longer period of time than RSPI after ice formation. A trend of hypoxic conditions subsequently spreading across the entirety of the pond from the deepest portion of RSPII was observed especially under winter ice cover. The production of total sulfides occurred simultaneously with the onset of hypoxia at depth in both open water periods with minor precipitation and ice covered conditions. However, the smell of H_2S was reported at RSPII only once the hypoxic conditions occurred within the entire water column during ice covered seasons; while no H_2S emission was reported at RSPI during the whole study period.

Statistics analysis indicates no significant correlation between DO and Chl-α or between DO and sBOD concentrations. However, characteristics of sBOD and DO still showed connection, especially during the lag period between open water and ice

covered conditions. In general, Chl-α concentrations were constant throughout the months of non-ice cover and no significant difference of Chl-α concentration at depths or locations (RSPI and RSPII) was observed due to the similarity of environmental conditions. However, RSPII experienced extremely high concentrations of Chl-α in ice covered conditions, and the species of blooming algae were successfully identified as *synurids*, *tabellaria*, and *asterionella* in the study. In both RSPI and RSPII, concentrations of sBOD were constant throughout the whole sampling period under ice covered and non-ice covered conditions.

Overall, the research raised more attention to the hypoxic conditions characteristics in SWPs and the maximum depth allowance in terms of SWPs design. Hypoxia occurs at depth and migrates if the conditions allow, which likely results in reduced water quality. As such, in a largely over-designed SWP with long HRT, excessive pond depth promotes the conditions of hypoxia, leading to a perfect environment for H_2S production.

References

Ampe, E. M., Bresciani, M., Salvadore, E., Brando, V. E., Dekker, A., Malthus, T. J., Jansen, M., Triest, L. and Batelaan, O. (2014). A wavelet approach for estimating chlorophyll-α from inland waters with reflectance spectroscopy. *IEEE Geoscience and Remote Sensing Letters*, 89-93.

Abdo, M. (2005). Physico-chemical characteristics of Abu Za'baal ponds. *Egyptian Journal of Aquatic Research* , 1-15.

APHA American Public Health Association. (2012). *Standard Methods for the Examination of Water and Wastewater, 22nd Edition.* APHA, WEF, AWWA.

ASCE American Society of Civil Engineers. (1989). *Sulfide in Wastewater Collection and Treatment Systems.* ASCE.

Bertilsson, S., Burgin, A. and Cayelan, C. (2013). The under-ice microbiome of seasonally frozen lakes. *Limnol Oceanogr*, 1998-2012.

DeLorenzo, M. E., Thompson, B., Cooper, E., Moore, J. and Fulton, M. H. (2012). A long-term monitoring study of chlorophyll, microbial contaminants, and pesticides in a coastal residential stormwater pond and its adjacent tidal creek. *Environ Monit Assess*, 343–359.

Hawley, N., Johengen, T.H., Rao, Y.R., Ruberg, S.A., Beletsky, D., Ludsin, S.A., Eadie, B.J., Schwab, D.J., Croley, T.E., and Brandt, S.B. (2006). Lake Erie hypoxia prompts Canada-U.S. study. *Eos, Transactions American Geophysical Union*, 313-319.

Horner, R. R., May, C. W. and Livingston, E. H. (2003). *Ecological effects of stormwater and stormwater controls on small streams.* Watershed Management Institute, Inc.

Hvitved-Jacobsen, T., Johansen, N. B. and Yousef, Y. A. (1994). Treatment Systems for Urban and Highway Run-off in Denmark . *The Science of the Total Environment*, 499-506.

Jaud, T., Dragon, A-C., Garcia, J. V., Guinet, C. (2012). Relationship between Chlorophyll a Concentration, Light Attenuation and Diving Depth of the Southern Elephant Seal Mirounga leonina. *PLOS one*.

Johnson, R. L., Holmquist, D., Redding, K. and McDaniel, C. (2015). *Water Quality with Vernier.* U.S.: Vernier Software & Technology.

Klein, R. (1979). Urbanization and stream quality impairment. *Water Res. Bull*, 948-963.

Kristiansen, J. (1975). On the Occurrence of the Species of Synura(Chrysophyceae). *Verhandlungen Internationale Vereinigung Limnologie*, 2709-2715.

Larson, G. L. (2000). Chlorophyll maxima in mountain ponds and lakes, Mount Rainier National Park, Washington State, USA. *Lake and Reservoir Management* , 333-339.

Leppi, J. C., Arp, C. D. and Whitman, M. S. (2016). Predicting late winter dissolved oxygen levels in Arctic Lakes using morphology and landscape metrics. *Environmental Management*, 463-473.

Marsalek, P. M., Watt, W. E., Marsalek, J. and Anderson, B. C. (2003). Winter operation of an on-stream stormwater management pond. *Water Science and Technology*, 133–143.

Mérette, M. R. (2012). *Primary production and nutrient dynamics of urban ponds.* Ottawa,Ontario, Canada: University of Ottawa, Faculty of Science.

Mischke, C. C. (2014). Winter Pond Fertilization Can Increase Phytoplankton Density in Aquaculture Ponds. *North American Journal of Aquaculture*, 76:67-71.

Muller, B., Bryant, L. D., Matzinger, A. and Wiiest, A. (2012). Hypolimnetic oxygen depletion in eutrophic lakes. *Environ Sci Technol*, 9964-9971.

OME Ontario Ministry of the Environment. (2003). *Stormwater management planning and design manual*. Queen's Printer for Ontario.

Robertson, D. M., Rose, W. J., and Saad, D. A. (2003). *Water Quality and the Effects of Changes in Phosphorus Loading to Muskellunge Lake, Vilas County, Wisconsin.* U.S. Geological Survey.

Shafi, A., Dogra, V., Gill, T., Ahuja, P. S. and Sreenivasulu, Y. (2014). Simultaneous Over-Expression of PaSOD and RaAPX in Transgenic Arabidopsis thaliana Confers Cold Stress Tolerance through Increase in Vascular Lignifications. *PLOS one*.

Samudro, G. and Mangkoedihardjo, S. (2010). Review on BOD, COD and BOD/COD ratio: a triangle zone for toxic, biodegradable and stable levels. *International Journal of Academic Research*, 235-239.

Semadeni-Davies, A. (2006). Winter performance of an urban stormwater pond in southern Sweden. *Hydrological Processes*, 165–182.

Stefan, H. G., Hondzo, M., Fang, X., Eaton, J. G. and McCormick, J. H. (1996). Simulated long-term temperature and dissolved oxygen characteristics of lakes in the north-

central United States and associated fish habitat limits. *American Society of Limnology and Oceanography,* 1124-1135.

Swistock, B. (2016). *Interpreting Water Tests for Ponds and Lakes.* The Pennsylvania State University. Retrieved from Penn State.

USEPA. (2009). *Stormwater wet pond and wetland management guidebook.* Ellicott City: United States Environmental Protection Agency.

Chapter 5

A Numerical Investigation on The Impact of Wind-induced Hydraulics on Dissolved Oxygen Characteristics in A Shallow Stormwater Pond

5.1 Setting the context

The article presented in this chapter is entitled *A Numerical Investigation on The Impact of Wind-induced Hydraulics on Dissolved Oxygen Characteristics in A Shallow Stormwater Pond* by Liyu Chen, Colin Rennie, Frances Pick, Alexandre Poulain, Patrick D'Aoust, Ru Wang, and Robert Delatolla. This article presents wind-driven currents in a stormwater pond (SWP) and the key findings of the influence of wind-driven circulation under different wind conditions on the spatial distribution of dissolved oxygen (DO) using a numerical model. The contributions of the authors' are as follows:

Liyu Chen: Conducted literature review, performed and optimized field sampling and experiment procedure, analyzed results, and wrote the manuscript.

Colin Rennie: Provided supervision in the development of research procedure, analysis of results, and revision of the manuscript.

Frances Pick: Provided expertise, supervision and guidance.

Alexandre Poulain: Provided expertise, supervision and guidance.

Patrick D'Aoust: Provided assistance in the collection of samples.

Ru Wang: Provided assistance in the collection of samples.

Robert Delatolla: Provided supervision, analysis of results, and revision of the manuscript.

5.2 Introduction

Wet stormwater ponds (SWPs) are widely used for flood and water quality control as one of the best management practices to mitigate the impact of runoff from highly urbanized areas (USEPA, 2009; MOE, 2003). SWPs are commonly designed to be shallow enough to prevent anaerobic digestion and thermal stratification, yet ensure enough depth to minimize algal blooms or resuspension of bed materials by major storm events (USEPA, 2004). A mean depth of approximately 1.00 to 3.00 is considered appropriate to provide acceptable environment and sufficient hydraulic retention time (HRT) (USEPA, 2004). Considerable literature to date has demonstrated that shallow water systems are susceptible to wind effects by previous field investigations (e.g., Kachhwal et al., 2012; Józsa, 2014) and laboratory studies (Liang et al., 2006; Pattantyus-Abraham et al., 2008; Bentzen et al., 2008; Fabian and Budinski, 2013). In SWPs, where minimal inflow is the normality, wind-driven flow can be the dominant hydrodynamic force in most of the non-ice covered periods (Pang et al., 2015; Andradóttir and Mortamet, 2016). The momentum of the wind is partially transferred into the water column to produce waves, turbulence and large scale circulation, whose generation does not require strong winds but may be generated by moderate winds. In particular, recent SWPs hydraulic studies show wind-driven flow speed and direction change with depth and that external surface forces are more efficiently transferred to the bottom of shallower ponds (Józsa, 2014; Andradóttir and Mortamet, 2016). Three dimensional methods were acquired in this study due to the inability of traditional two-dimensional depth-averaged computational methods predicting variation in depth of wind-generated current speed and direction.

The captured runoff is retained for an appropriate duration of time and mitigated through physical, chemical and biological processes within stormwater

facilities (Behera and Teegavarapu, 2015). Good water quality in these ponds is essential not only to preserve the quality of the downstream receiving environments but also to ensure adequate aquatic habitats in wet facilities (Marsalek et al., 2005b). The vast majority of stormwater quality studies have evaluated chemical and biological characteristics. Although some studies demonstrate the significance of hydraulic efficiency on SWPs with respect to pond shape, boundary configurations and topography (Jansons and Law, 2007; Glenn and Bartell, 2010; Zounemat-Kermani et al., 2015), very few studies have investigated the correlation between wind-driven hydraulic performance and detained stormwater quality. Dissolved oxygen (DO) is essential to the ecological environment and treatment performance in SWPs, which can be strongly affected by waves, turbulence and large scale circulation. As such, in wind-induced flow dominated SWPs, wind characteristics likely influence pond hydraulics and subsequently the DO spatial distribution and stratification. The objective of the present study is to evaluate the influence of wind-driven circulation on the spatial distribution of DO in a SWP using numerical model.

Most previous DO computational models have considered SWPs to be completely mixed compartment due to shallow bathymetry (Wium-Andersen et al., 2012). However, as will be shown, in the present study, DO concentrations varied significantly in the water column from surface to bottom of the studied pond, and complete mixing appeared only during a short period of time. Due to the complexity of wind-driven flow affecting DO concentrations at different depths, the assumption of 'complete mixing' of the SWPs was not suitable for this study.

Many previous studies have simplified simulation of the oxygen cycle in ponds and rivers. For example, Wium-Andersen et al. (2013) considered only photosynthesis/respiration and sediment oxygen demand (SOD), and Fan and Wang

(2008) took only the process of biological oxygen demand (BOD) into consideration. However, DO is connected to many environmental processes and parameters such as reaeration, photosynthesis/respiration, SOD, degradation of organic matter (e.g. BOD) and nutrient cycling. Moreover, these processes are likely specific to certain locations in the ponds and the various parameters may vary spatially. Hence, a more complex model that incorporates all of the above listed processes and parameters was required in this study.

In order to study wind-generated hydraulics and its influence on DO concentrations, a three-dimensional computational model was developed using MIKE 3 FM (DHI software) for wind-driven hydrodynamics coupled with the ECOlab add-on. The advantage of full three-dimensional simulation with MIKE 3 is that it allows computation throughout the whole water column so that different characteristics, such as current speed/direction and DO concentrations, can be produced at different depths. ECOlab simulates DO concentrations over time based on a certain hydrodynamic condition, considering the influence of reaeration photosynthesis/respiration and oxygen consuming substances, such as BOD, SOD and nutrient cycling of ammonia, nitrite, nitrate and phosphorus.

The present study was conducted in a SWP in Ottawa, Canada. The hydrodynamic model was validated using velocity measurements taken by an acoustic Doppler current profiler (aDcp). To the best of the authors' knowledge, the stationary velocity measurements provided by a bottom-mount aDcp were used the first time to collect small wind-induced currents in a SWP. The water quality model was calibrated and validated using *in-situ* samples taken on the same day as the velocity measurements. The major contributions of the study include: i) visualized three-dimensional aDcp current results in a SWP given the constraint of fairly small

magnitudes; ii) three-dimensional wind-induced current and DO concentration simulation in a SWP using MIKE 3 and ECOlab with convincing validated speed and direction; iii) an assessment of DO concentrations characteristics under different wind speed conditions.

5.3 Materials and Methods

5.3.1 Study site description

The study was conducted at Riverside Stormwater Pond II (RSPII), a 45,000 m^2 fresh water pond in a residential area of Riverside South, Ottawa, Canada. The pond was constructed in 2005, and is operated by the City of Ottawa. *Figure 5.1* shows the bathymetry of RSPII as well as the locations of the measured aDcp stationary data points and DO sampling locations. The facility contains a large forebay with a maximum depth of 1.60 m, and the main body of the pond includes a 2.20 m deep trench extending from the southern end of the pond to the outlet. The inlet is located at the south-east end of the pond with an average annual discharge of $0.003 m^3/s$. The HRT of RSPII, depending on the amount of precipitation and inflow, can range from 15 days to 125 days. The pond drains into a creek at the north of the facility, close to where the outlet is located. Periodic events of H_2S emission have been reported since 2009, coinciding with periods of summer droughts and winter ice cover, during which lesser water quality was also demonstrated. These events are associated with hypoxic conditions near the bed, thus understanding of mixing patterns in the pond is essential for mitigation of H_2S production.

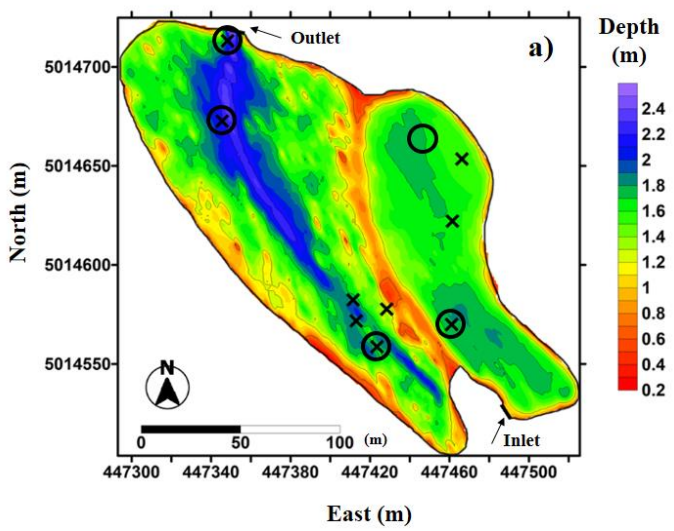

Figure 5.1 aDcp data collection locations (x symbols) and DO sampling locations (circles) at RSPII on August 25th, 2015 with RSPII bathymetry (domain used in MIKE 3 FM model)

5.3.2 The acoustic Doppler current profiler (aDcp) data collection

Velocity measurements were performed using a SonTek RIVERSURVEYOR® M9 (San Diego, CA) aDcp. This instrument was chosen due to its ability of real-time currents velocity collection within the whole water column. Detail description of aDcp working techniques and terminology can be found in (Simpson, 2001).

Velocity measurements in the study were acquired on August 25th, 2015 between 11:00 and 16:00 at RSPII using the M9 aDcp at the sampling locations shown in *Figure 5.1* . Due to the expected very low flow velocities at RSPII, measurement noise caused by boat movement can cause masking effects. To rectify this issue, a stationary bottom-mounted system was utilized for velocity data collection in this study. A Magellan ProMark3 Thales GPS unit with antenna (Santa Clara, CA) was used to record sampling locations. During velocity data collection, the aDcp unit was sitting at the bottom recording velocity profile from 0.45 m above the bottom and the boat was driven at least 2 m away from the collecting locations to mitigate the effect

of boat movement on current velocity. Velocity profiles were recorded for approximately 600 s at each location with vertical resolution ranging from 0.02 to 0.06 m. One challenge of bottom-mounted collection in a natural pond was vegetation. Sampling locations were carefully selected, and data were monitored in real-time, to avoid potential for macrophytes covering or disturbing the aDcp transducers.

A MATLAB code developed by Rennie (Kachhwal et al., 2012) was modified and applied to process, and filter time and space average raw data to obtain mean velocity and direction within 10 cm depth cells in the water column. The aDcp data provides a visualized three-dimensional flow velocity profile at various depths, which helps to understand the circulatory patterns in RSPII under certain weather conditions.

5.3.3 Wind data collection

Wind speed and direction were obtained at RSPII on August 25th, 2015 using a HOBOware U30 Station wind logger (Bourne, MA) with a collecting frequency of 10 s. The wind anemometer was located at the inlet structure and securely fastened to a permanent railing at approximately 10 m above the water surface in order to minimize wind disturbances. Collected wind data were also compared and confirmed using climate data provided by Ottawa International Airport which is located approximately 4 km from RSPII.

5.3.4 Water quality sample collection

Water quality data of DO, BOD, chlorophyll-α (Chl-α), ammonia, nitrite, nitrate and total phosphorus (TP) were needed as model inputs in this study. All samples measurements used in this study were acquired at RSPII at four specific depths (0.50 m, 1.00 m, 1.50 m and 2.00 m below the water surface) where it is feasible on the same day and across the same general time period as the velocity and

wind measurements. DO concentrations were taken *in-situ* using a field optical YSI ProODO DO meter (Yellow Springs, OH). Water samples for BOD, COD, Chl-α, ammonia, nitrite, nitrate and TP testing were collected using a Wildco 1520 C25 Kemmerer Bottle 2.2L TT water sampler (Yulee, FL). Tests were conducted using standard methods, as outlined in Table 5-1. BOD and COD analyses were performed on the same sample across a total of 18 samples to establish a BOD/COD ratio. This ratio was used to convert subsequent COD measurements to BOD values to benefit from the higher accuracy of COD analytical techniques.

Table 5-1 Testing methods used for water quality parameters (American Public Health Association, 2012)

COD	Hach Method 8000 (equivalent to Standard Method 5220 D)
BOD	Modified Standard Methods 5210B
Chl-α	Modified Standard Methods 10200 H (with 95% Ethanol extraction)
Ammonia	Hach Method 10205 (equivalent to Standard Method 4500-NH_3-B)
Nitrite	Standard Methods 4500-NO_2-B
Nitrate	Standard Methods 4500-NO_3-B
TP	Hach Method 8190 (equivalent to Standard Methods 4500-P E)

5.3.5 Laboratory kinetics study

Sediment samples were collected at RSPII outlet using an Ekaman dredge for laboratory kinetics testing. Laboratory results of BOD bottles experiments were utilized to determine the rates of change values, Arrhenius temperature coefficient and half-saturation constants that were used as inputs for the MIKE 3 FM ECOlab model. Sediment samples for the experiments were harvest from the outlet of RSPII during fall of 2015. The Arrhenius temperature coefficient was determined for SOD and nitrification by analyzing kinetics data acquired during laboratory testing. By plotting

the change per unit of time of constituents over time (day), the rate of change values of DO and ammonia concentrations can be obtained at 20 °C. The BOD, SOD and nitrification rates of change were plotted against DO and the resulting curve was utilized to determine half-saturation coefficients, which was outlined by Ghimire in 2012.

5.4 Numerical model development

5.4.1 Hydrodynamic and water quality module

The three-dimensional hydrodynamic model MIKE 3 FM by DHI software (MIKEbyDHI, 2012) was applied for RSPII pond flow simulation. MIKE 3 flow model FM is developed for applications within oceanographic, coastal and estuarine environment. Based on the small velocities inherent to RSPII, wind-driven flow may significantly contribute to the velocity profile of the pond. The model was chosen based on the capability of simulating three-dimensional flow throughout the entire water column. Detailed information of the hydrodynamic model can be found in MIKEbyDHI-MIKE 21 & MIKE 3 Flow Model FM Scientific Documentation (2012). The hydrodynamic model is based on the numerical solution of three-dimensional incompressible Reynolds averaged Navier-Stokes equations invoking the assumptions of Boussinesq and hydrostatic pressure. In this study, sigma-coordinates were used for the vertical mesh, where a σ-transformation was used for velocity components. Boundary shear stress was derived from the log-law. A cell-centered finite volume method was used for spatial discretization performance. The turbulent kinetic energy and the rate of dissipation of the turbulent kinetic energy are acquired from the $k-\varepsilon$ model (Rodi, 1984). The eddy viscosity is calculated locally from $k-\varepsilon$. The model is capable of taking into consideration wind stress,

evaporation/precipitation, and the open boundaries can be defined using speed or elevation. Wind stress is developed on a drag formula (Wu, 1980; Wu and Tsanis, 1994) based on wind speed.

Water quality was modelled using MIKE 3 FM ECOlab (MIKEbyDHI, 2016), which is a numerical model for three-dimensional ecological modelling based on a specific hydrodynamic condition. The model describes processes and the physical, chemical and biological interactions among ecosystem state variables, including the physical process of sedimentation of state variables, and it is coupled to the Advection-Dispersion Modules of the DHI hydrodynamic flow models, so that transport mechanisms based on advection-dispersion can be integrated in the ECOlab simulation (MIKEbyDHI, 2016). In this study the model is used to assess the impact of wind-driven advection-dispersion on DO conditions, and in this specific model, oxygen balance is described as a function of reaeration, the biotic processes of photosynthesis and respiration, degradation of organic matter (decay of BOD), and the interaction with sediment (SOD) and nutrient cycling (nitrification of ammonia to nitrite and nitrite to nitrate). A general relation between DO and control parameters can be described as

$$DO = reaeration - nitrification - BOD + photosynthesis - respiration - SOD$$

Detail information of the water quality model can be found in MIKEbyDHI-Water Quality WQ Templates ECOlab Scientific Description (2012).

5.4.3 MIKE 3 model configuration and implementation

In order to simulate wind-driven flow in RSPII using MIKE 3 FM, a triangular computation mesh was generated coupled with 10 unevenly spaced z-levels (layers), and boundary characteristics. Open boundaries were manually designated at the inlet

and outlet based on the bathymetry and coordinates of inlet and outlet structures of RSPII.

Annual discharge of 0.003 m^3/s was set for the inlet and outlet of the pond based on stage of the pond during the field investigation. The pond boundary was set as a land boundary where normal velocity is equal to zero. To maintain the permanent pool level at the SWP conditions, a 4.00 m width by 0.50 m height trapezoidal weir with bottom width of 2.00 m was created at 2.00 m above the bed to retain similar water level in the system at the outlet boundary, where fluid entry through the boundary was prevented. A horizontal 1.00 m diameter circular culvert was set up at 0.50 m above the bed to simulate the inlet condition. The initial hydrodynamic conditions in the model were applied using the final stage condition of a preliminary run without wind add-on. Density was defined as a barotropic fluid. Wind speed and direction were applied using data collected on the same day as the aDcp measurements within the whole running period from 7:00:00 to 16:43:20 August 25th, 2015. The drag coefficient of wind in this model was calibrated based on Geemaert and Plant (1990). Precipitation was estimated using data from Ottawa International Airport weather station (CCN, 2016) and evaporation were acquired from Ferguson et al. (1970). In total, the model was run with 3500 time steps and time interval of 10 s. Mesh and time step independence study was implemented, and with this specific setup, the Courant number was approximate 0.02, which was within the software recommended value (MIKEbyDHI, 2007). Table 5-2 shows more detail information of domain characteristics.

Table 5-2 MIKE 3 domain characteristics

Parameters	Model input
Elements	2118.0
Nodes	1138.0
Precipitation	4.0 mm/day
Evaporation	9.6×10^{-1} mm/day
Wind friction	2.0×10^{-3} N/m^2

The ECOlab model simulates DO characteristics based on the biochemical interaction of BOD, Chl-α, ammonia, nitrite, nitrate and TP. To simulate the environmental processes, ECOlab acquired initial conditions, boundary conditions along with kinetics and parameters as inputs. Water quality measurements at RSPII on August 25th, 2015 were set as initial conditions to initiate the run of model. Likewise, boundary conditions of concentrations of water quality parameters were based on *in-situ* samples in proximity to the inlet and outlet at RSPII. Measured concentrations of BOD, ammonia, nitrite, nitrate and TP on the simulation day were entered as initial and boundary conditions (Table 5-3). The concentrations of these parameters are constant seasonally, which indicates representative of conditions at RSPII. The model does not simulate macrophytes at the bed and in proximity to the border, which could contribute to DO concentration fluctuation through photosynthesis and respiration. As such, Chl-α concentrations were adjusted to higher values (shown in Table 5-3) for both initial and boundary conditions to simulate the contribution generated by macrophytes on August 25th, 2015 at RSPII. Inflow concentration of Chl-α was set to the seasonal average of 0.02 mg/L of RSPII; Initial condition and outlet condition were adjust to 0.60 mg/L and 0.20 mg/L to compensate the inadequacy of photosynthesis and respiration from vegetations. However, it needs to be mentioned that no literature has been found to support this assumption specificly

for MIKE 3 Chl-α inputs. Values of state variables of both initial condition and boundary condition are listed in Table 5-3

Some of the essential constants of environmental processes in MIKE 3 ECOlab were retrieved from laboratory experiments. The soluble biochemical oxygen demand (sBOD) remained low and constant throughout the whole study period with a first decay rate of 0.48 mg/L per day at 20 °C obtained in lab, which was similar as the value reported by Tu et al. (2014) on a constructed wetland in Taiwan. The half-saturation oxygen concentration of sBOD was 1.37 mg/L. Nitrification is modeled as the process of ammonia oxidation to nitrite and nitrite oxidation to nitrate. First decay rate of overall nitrification of 0.17 mg/L per day at 20 °C was acquired using lab experiment. The rate of ammonia oxidation of 0.17 mg/L per day is equal to the rate of nitrite oxidation of 0.17 mg/L per day since no nitrite accumulation occurred during the process. Comparing to Tu et al. (2014), RSPII has a relatively low ammonia/nitrite removal efficiency. Moreover, temperature coefficient for nitrification decay rate of 1.088, temperature coefficient for SOD of 1.15, along with half-saturation oxygen concentration of nitrification and SOD of 0.48 and 3.51 mg/L were obtained from lab respectively.

SOD is composed of chemical SOD and biological SOD (Wang, 1980). It is evident that the biological activity various geographically and spatially due to the different sediment conditions. To account the availability of spatial distributed carbon in sediment, the SOD per m^2 parameter was varied spatially to incorporate the mass flux of carbon into the kinetic rate. Therefore, higher values of SOD per m^2 of 3.00 to 5.00 g/m^2/ day was retained in the forebay due to the higher carbon input contributed by abundant sedimentation (USEPA, 2004) and population of microorganisms (Wang, 1980). Likewise, lower SOD per m^2 of 0.00 to 2.00 g/m^2/ day was generated in the

main body according to the lab result of 1.75 g/m^2/day obtained from water samples in main pond. This assumption was furthermore supported by literatures. Rong and Shan (2016) reported SOD per m^2 (20°C) of two rivers in China ranged from 0.0 to 2.0 g/m^2/day. A lake in Illinois, US stuied by Butts and Evans (1979) showed higher SOD (20°C) between 2.0 and 7.0 g/m^2/day.

Water transparency is essential to algae populations within water column, and Secchi disk depth is a commonly used parameter to characterize optical properties (Tilzer, 1988). Spatially non-uniform Secchi disk depths proved importance in successful modelling of the complex spatially variable environmental conditions of RSPII. According to Jamu et al. (1999), Chl-α showed a negative correlation with Secchi disk depths due to its positive linear regression with overall light extinction coefficient. Secchi disk depths were assumed with an average of 0.50 m in the forebay, and around 1.80 m in the main body, considering the change of turbidity due to different concentrations of sediment within water column.

Photosynthesis and respiration processes were described relative to a given maximum production at noon and the respiration rate. The ratio of maximum oxygen demand at noon versus respiration rate of plants of approximately 3:1 was obtained from Mérette (2012), and the values were set as 10 g/m^2/day for maximum production at noon and 3 g/m^2/day for respiration rate. Essential constants of DO model including default values and values obtained and validated using lab results and literatures are listed in Table 5-4.

Table 5-3 Initial and boundary inputs of ECOlab simulation in MIKE

Variable	Initial condition (mg/L)	Inlet boundary (mg/L)	Outlet initial condition (mg/L)
DO	10.0	10.0	10.0
BOD	1.0	2.0	2.0
Chl-α	6.0×10^{-1}	2.0×10^{-2}	2.0×10^{-1}
Ammonia-N	5.0×10^{-2}	5.0×10^{-2}	5.0×10^{-2}
Nitrite-N	9.0×10^{-4}	5.0×10^{-4}	5.0×10^{-4}
Nitrate-N	7.0×10^{-1}	8.0×10^{-1}	8.0×10^{-1}
TP	2.0×10^{-2}	2.0×10^{-2}	4.0×10^{-2}

Table 5-4 Essential constants of environmental processes in MIKE 3 ECOlab

Description	Values	Source
Oxygen processes		
Temperature coefficient for respiration	1.08	Default
Half-saturation coefficient for respiration	2.00 mg/L	Default
Temperature coefficient for SOD	1.15	Measured
Half-saturation coefficient for SOD	3.51 mg/L	Measured
SOD per m^2	Spatially distributed	Measured/ Calibrated
Maximum oxygen production at noon, m^2	10 /day	Calibrated
Respiration rate of plants, m^2	3 /day	Calibrated
Secchi disk depths	Spatially distributed	Calibrated
BOD processes		
1^{st} order decay rate at 20 °C (dissolved)	0.48 /day	Measured
Temperature coefficient for decay rate (dissolved)	1.07	Default
Half-saturation oxygen concentration	1.37 mg/L	Measured
Nitrification		
1^{st} order decay rate at 20 °C for ammonia to nitrite	0.17 /day	Measured
1^{st} order decay rate at 20 °C for nitrite to nitrate	0.17 /day	Measured
Temperature coefficient for decay rate	1.088	Measured
Half-saturation oxygen concentration	0.48 mg/L	Measured
Oxygen demand by ammonia oxidation	3.42 g O_2/g NH_4-N	Default
Oxygen demand by nitrite oxidation	1.14 g O_2/g NH_4-N	Default
Chl-α processes		
Carbon to oxygen ration at primary production	0.2857 mg C/mg O	Default

5.5 Results and discussion

5.5.1 In-situ aDcp collected flow coupled with wind measurements

Understanding of wind-induced flow in SWPs is necessary to understand mixing processes that influence water quality. *Figure 5.2* shows wind speed and direction within the aDcp sampling period from 7:00 to 18:00 at RSPII on August 25th, 2015. An average wind speed of 2.30 m/s and direction of 229.00° were observed. Comparing with the historical wind data from the Ottawa International Airport, moderate wind speed was collected on August 25th, 2015. In this study, a high-wind day and a low wind day were defined as average wind speed of 4.30 m/s and 1.10 m/s according to historical data of 2015 measured within the same time range as aDcp measurements.

The bathymetry data of RSPII used in this study was provided by a bottom tracking collection of preliminary boat-mounted aDcp measurements acquired by the City of Ottawa on May 23rd, 2013. *Figure 5.3* demonstrates three-dimensional vector plots of aDcp-measured current velocity and direction at RSPII on August 25th, 2015 with bathymetry and an approximate average wind direction viewed in different angles. Easting and northing are presented as x and y axis, and z axis represents pond depth in this figure. The measured velocities show an average magnitude around 1.00 cm/s at all locations at RSPII, with standard error in measured horizontal velocities less than 0.10 cm/s. A study on Lake Okeechobee, Florida, USA (Jin and Ji, 2004) reported the wind-produced flow velocity can range from 0.00 to 40.00 cm/s in a lake with an approximate depth of 2.70 m with an average wind speed of 5.00 m/s. Moreover, Kachhwal et al. (2012) demonstrated that with average wind speed more than 7.00 m/s, a velocity magnitude of order 5.00 cm/s can be generated in the Shebandowan Mine tailings storage facility, Ontario, Canada, where only wind-driven

flow existed. Although the collected current velocities were generally small in this study, velocity magnitude at RSPII falls within similar order as those of Lake Okeechobee and the Shebandowan Mine tailings pond.

Currents near the water surface (*Figure 5.3*) were observed to be in the downstream direction of the wind. This suggests wind conditions on August 25th, 2015 generated enough momentum to generate surface current moving downwind. Wind-induced currents gradually changed direction towards the pond bottom (*Figure 5.3*), indicating complex circulation patterns were created at different depths due to a non-linear interaction between currents (Signell et al., 1990). Moreover, counter-current flow in the opposite direction was observed near the bottom at some locations. Higher velocities were mainly observed close to the surface of the pond. Velocities collected close to the outlet facility of RSPII were smaller at all depths (less than 0.50 cm/s), where higher and more constant velocities were expected due to the discharge. These observed characteristics of velocity magnitudes and current directions support the assumption of wind being the only important driving force of flow at RSPII during non-ice covered conditions. Both the studies of Dumas et al. (2012) and Dufresne et al. (2014) suggest that wind directions are essential to driving overturning circulation that leads to efficient mixing. The aDcp results demonstrate significant influence can be created on mixing in RSPII under the wind directions on August 25th, 2015. In the Ottawa region, more than 50 percent windy days (defined as daily maximum wind speed over 8.60 m/s) were with wind directions from 170° to 290° between May and October, 2015 measured at Ottawa International Airport, which means with dominated southwestern wind, an effective impact of wind on flow current at RSPII can occur during the summer period.

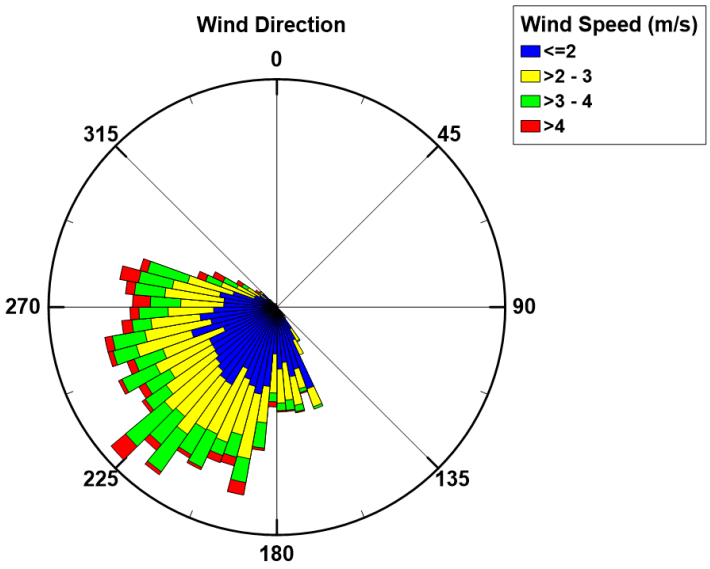

Figure 5.2 Wind speed and direction during aDcp data collection measured at RSPII

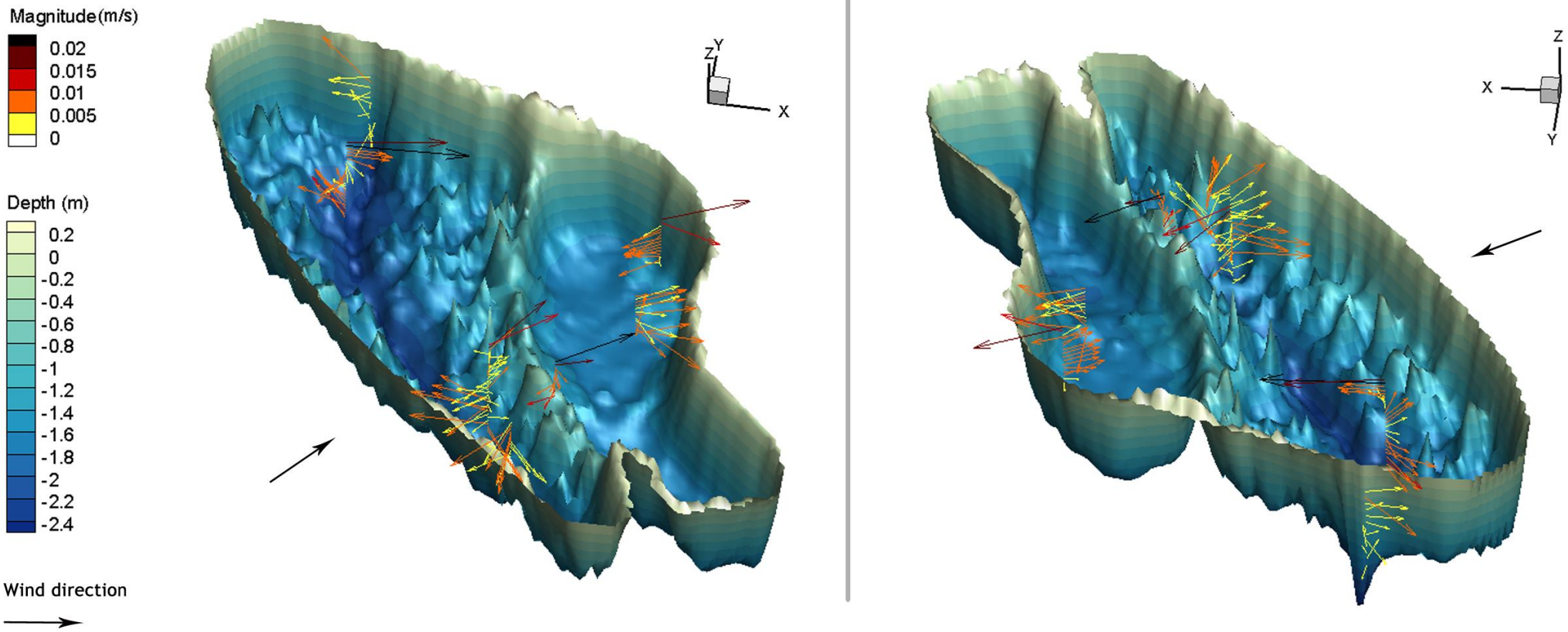

Figure 5.3 Three-dimensional visualization of velocity magnitude and direction pattern of current flow at RSPII with bathymetry and an approximate average wind direction viewed from different angles

5.5.2 Model validation and verification

Simulated results of hydrodynamic model were validated using the aDcp-measured flow data on August 25th, 2015 at RSPII. Both linear regressions and functional relations are presented in this paper. *Figure 5.4* illustrates a reasonable agreement between sampled and simulated values of velocity magnitudes and a good agreement between the sampled and simulated values of flow directions. Although the regression coefficient of determination (r^2) of velocity magnitude was small, the lower and upper 95% confidence slopes of 0.33 and 0.69 still showed a significant correlation between the observed and simulated velocity magnitudes (*Figure 5.4 a*). *Table 5-5* shows the statistics of the correlation plots. Given that the velocity magnitudes of both observed and simulated results were very small, the mean absolute velocity error (ε_a) of velocity correlations seemed reasonable. The average discrepancy ratio (d) was 1.62, which showed a general over-prediction (positive bias) of simulated velocity magnitude. Although under-prediction was observed with lower velocity magnitudes while over-prediction occurred with higher velocity magnitudes, approximately 84% velocity magnitudes fell within $0.75<d<1.33$. Linear regressions assume that all error occurs in the *y* variables by minimizing the sum of square errors vertically from the regression line, while a principal axis functional relation describes the relation between *x* and *y* variables by minimizing the error on both axis (Rennie and Villard, 2004). *Figure 5.4 a* demonstrates that a functional relation better describes the relation between observed and simulated velocity magnitudes. The functional relation slope was greater than 1:1 by 45°, which supports the finding of over estimation of larger velocity magnitudes.

The linear correlation of flow directions had a better correlation than velocity magnitudes with a higher r^2 and 95% confidence upper slope of 1.01 along with 0.70

lower slope (*Figure 5.4 b*). Both ε_a and the root mean error (ε_{rms}) were less than 40% of the mean flow direction. Moreover, the mean discrepancy ratio (d_{avg}) was 1.29 and more than 85% of the velocity directions were within the range of 0.50<d<2.00. The functional relation slope of wind direction was fairly close to 1, demonstrating a well-correlated relation was established between observed and simulated results. In proximity to the pond surface, more than half of the sampling locations, both observed and simulated velocity directions ranged from 15 to 55°, were in the downstream direction of the wind. An average velocity direction of 200° was observed at depth, which indicated that counter-current flow occurred near the bottom of the pond. Overall, the model was capable of simulating extremely small flow and wind-produced current at RSPII.

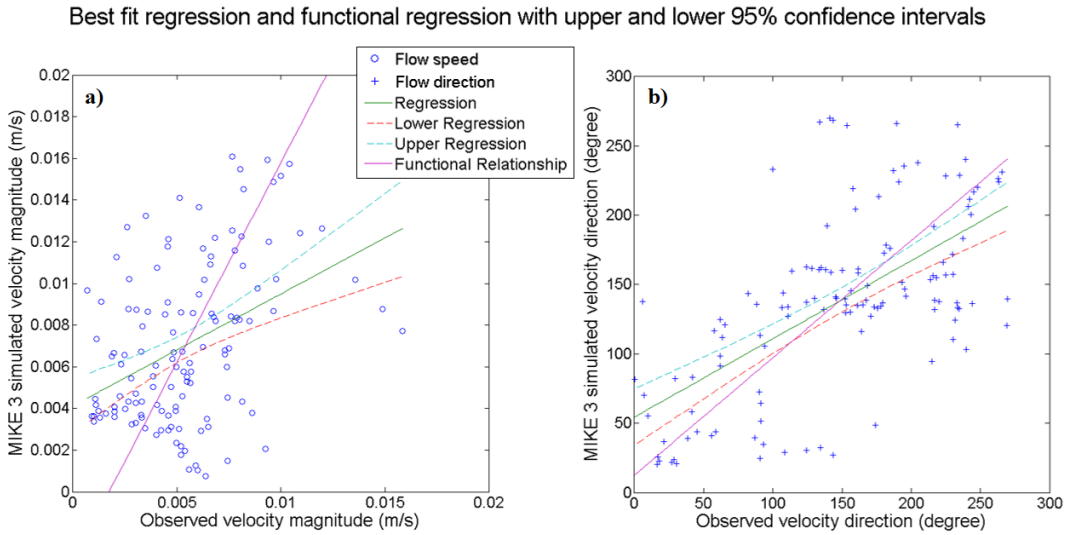

Figure 5.4 Scatter diagrams of observed versus simulated a) velocity magnitudes and b) flow directions with linear regression and functional relation. Upper and lower 95% confidence bounds on the regressions are shown by dashed lines.

Table 5-5 Statistics analysis of observed against simulated velocity magnitudes and flow directions

Measured vs. Simulated	r^2	ε_a	ε_{rms}	d_{min}	d_{max}	d_{avg}	Percentage (%) 0.5<d<2.0	Percentage (%) 0.75<d<1.33
Velocity magnitude (m/s)	0.17	0.0032	0.0041	0.12	6.57	1.62	0.89	0.84
Velocity direction (degree)	0.39	41.57	60.08	0.19	23.34	1.29	0.86	0.52

The water quality model was validated using DO readings collected on August 25th, 2015 and the results are shown in color maps interpolated and plotted using Surfer® 11 by Golden Software, LLC (*Figure 5.5*), where high concentration of DO is indicated as red and low concentration of DO is indicated as purple. Although limited DO data were collected *in-situ* due to restricted sampling time for carrying out both velocity and DO measurements on the same day, a very strong correlation was still established as demonstrated by r^2 of 0.70 (*Figure 5.6*). Both underestimations and overestimations were generated with higher DO concentrations due to the difficulty and complexity of environmental processes modelling, such as the non-homogenous water environment, over simplified description of mathematical formulations, and the uncertainty of vegetation simulation. However, linear regression slope and functional relation slope of 0.98 and 1.22 respectively, showed a very good prediction of DO through ECOlab.

The locations of velocity and DO concentration measurements were recorded with a nominal horizontal position accuracy of 0.005 m using a Magellan ProMark3 Thales GPS, although boat drift along the mooring line during data collection increased positioning uncertainty. Also, vegetation at the bottom of RSPII made data collection challenging, especially for velocity data collection using a bottom-mounted aDcp. As such, it should be acknowledged that uncertainties were involved in the observed data. For water quality model, even though some of the constants input of

environmental processes were calibrated using experimental data and literature values, uncertainties still existed due to the unique environment of RSPII. Regardless, overall the model validation was satisfactory, suggesting the model can be applied to evaluate mixing under various wind conditions.

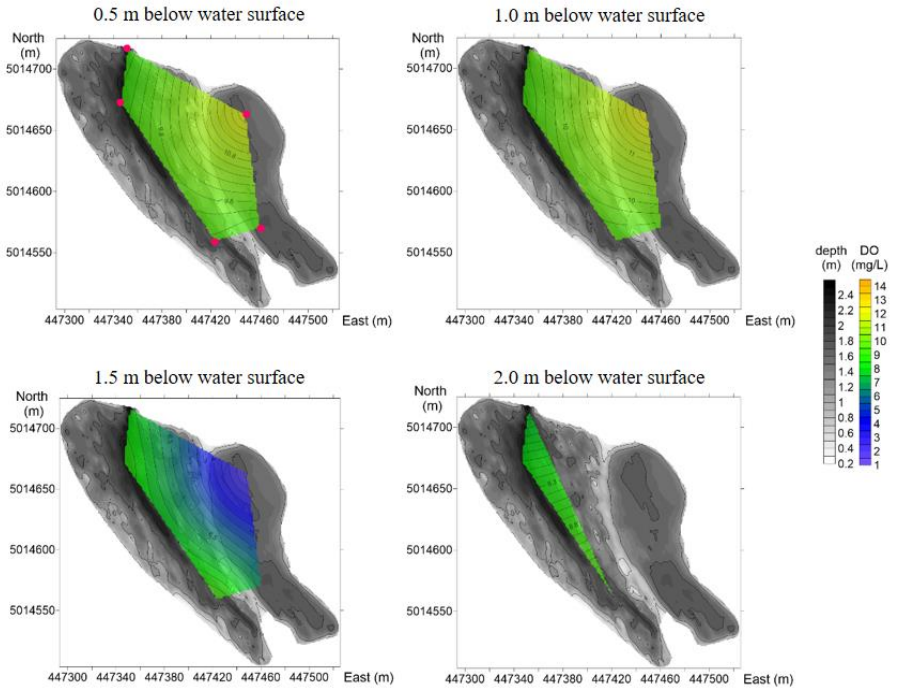

Figure 5.5 DO concentrations at five locations at 0.5 m, 1.0 m, 1.5 m and 2.0 m below the water surface at RSPII on August 25th, 2015

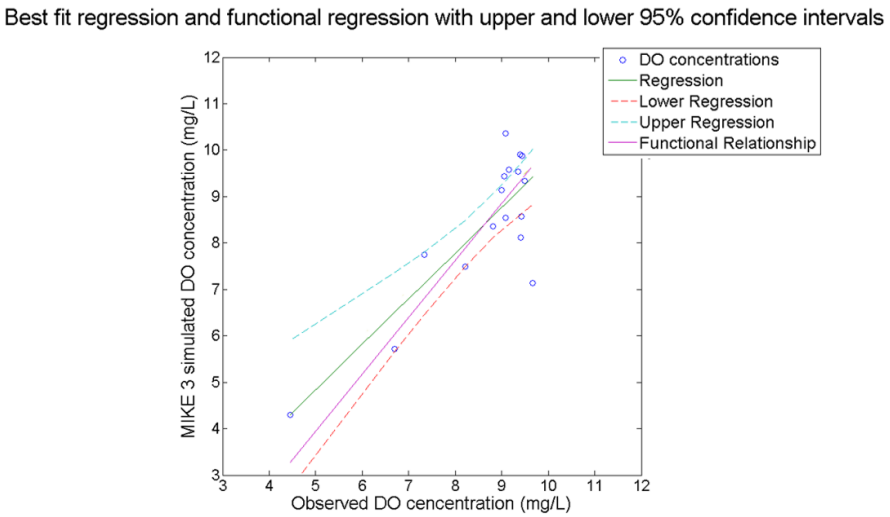

Figure 5.6 Scatter diagram of observed versus simulated DO concentrations with linear regression and functional relation; perfect agreement is shown as dash line

5.5.3 Numerical flow simulation

Figure 5.7 illustrates simulated velocity magnitudes and directions at four specific layers at RSPII. In the σ-coordinate system, MIKE 3 generates layers evenly in the vertical at each mesh cell depending on the total depth of each mesh cell. Consequently, layer thickness is smaller at mesh cells with less total water depth. Although the same layer doesn't represent the exact same depth in the figure, larger layer numbers indicate layers closer to water surface. For example, layer 10 stands for the layer that was closest to surface and, to the contrary, layer 1 represents the one that was in proximity to the bottom. At the surface layer, flow directions homogeneously correlated with downwind directions and larger velocity magnitudes were simulated due to wind friction. Wind had a stronger impact on shallower bathymetry (Coman and Well, 2012) and higher velocity magnitudes were observed at the surface at locations with smaller total water depth. Conversely, countercurrent flow in proximity to the bottom of the pond (layer 1) was oriented in the opposite direction to surface velocities due to energy maintenance and mass conservation (Wu and Tsanis, 1994). The MIKE 3 simulation of opposite directions of surface and bottom flow, similar to the aDcp observations, further suggests that wind-driven flow is the main current in RSPII in summer months because of the minimal inflow. Complex circulation cells were generated, especially below the surface layer (*Figure 5.7 b, c & d*), under certain wind conditions due to wind momentum, fluid viscosity, wave-current interaction, irregular bathymetry and abrupt depression (Kachhwal et al., 2012; Signell et al., 1990). With the upwelling current created by countercurrent flow at depth at the southeastern boarder, a pond scale upwelling circulation was produced by wind-driven flow, which indicates that hydrodynamic mixing was achieved by wind drive circulation.

Figure 5.8 a & d show that DO spatial distribution at both surface and bottom layers changed with wind-produced current at RSPII. A segment of higher DO concentrations around 9.00 mg/L was predicted from the south inlet to north forebay, along with the southeast pond due to better replenishing generated by spanwise flows close to the surface. Lower DO between 0.0 and 4.0 mg/L was simulated at depth in the main body of RSPII with exception of the area south of the outlet where near-bed circulation formed a circle of higher DO concentrations of 7.0 mg/L. Due to the downward current generated at the east border of the forebay, DO from the surface supplied the forebay bottom. To the contrary, low DO near the bed at the southwest was raised to the surface through the upward momentum created by pond scale circulation.

Under the same chemical and hydraulic setup, a low-wind day and a high-wind day (defined in section 5.5.1) comparing to August 25th, 2015 were modelled based on wind data collected from Ottawa International Airport. In light wind conditions with average wind speed of 1.15 m/s shown in *Figure 5.8 b & e*. Decreased wind speed had a greater impact on current directions than velocity magnitudes, which is supported by the findings of Andradóttir and Mortamet's (2016). Due to the decrease of wind speed, the overturning circulation weakened, which allowed the development of a stronger vertical stratification (Dumas et al., 2012) and caused hypoxic conditions, defined as DO concentration less than 2.00 mg/L, to be simulated at the bottom of the forebay. Low DO in natural lakes or ponds is likely due to decomposition of dead algae and aerobic microbial activities (Torno, 1985). With the lack of circulation, anaerobic conditions can be formed resulting in odor issues and reduced water quality. Under more intense wind conditions of 4.38 m/s average wind speed (*Figure 5.8 c & f*), higher flow speed was generated at both depths, and a stronger pond-scale

circulation was generated with downwind current at surface and countercurrent flow at depth. As such, DO stratification was prevented by stronger circulation, which was created by upwelling windward lower DO at depth and downwelling leeward higher concentrations of surface DO (Dumas et al., 2012). Although Andradóttir and Mortamet (2016) reported wind-produced vertical mixing, short-circuiting and basin scale mixing decreased mean residence time, which may have led to reduced water quality. The present model demonstrates that typical high wind conditions lead to full mixing, sufficient to eliminate hypoxic zones in proximity to the bed.

Figure 5.9 provides cross-sectional views of DO stratification along the crosswind direction under the three wind conditions. In the wind conditions on August 25th, 2015 (*Figure 5.9 a*), stronger countercurrent flow generated from downwelling current at the east border led to higher DO concentrations within the upper water column in the forebay. Comparing with the vertical profile under low wind conditions (*Figure 5.9 b*), lower DO concentrations were pushed towards the west bank through countercurrent flow at depth (*Figure 5.9 a*). Microalgae at 0.50 m depth have higher productivity with respect to photosynthesis (Sutherland et al., 2014). As such, higher DO was observed at depths ranging from 0.50 to 1.00 m in low wind conditions, where less mixing and stronger stratification occurred. *Figure 5.9 c* demonstrates a fully mixed cross-section in high wind conditions. Neither hypoxic conditions nor dead zones were observed even at depth. Stronger downwind current was produced at the forebay surface comparing to smaller wind speed conditions (*Figure 5.9 a*) which generated both larger downwelling flow in the forebay and stronger upwelling current at the west border in the main pond. The average DO concentrations in this fully mixing condition were around 7.00 mg/L at all depths. Hence, complete mixing is achievable by wind.

Overall, with the significant contribution of wind-induced current, hypoxic zones at depth can be prevented by upwelling circulation.

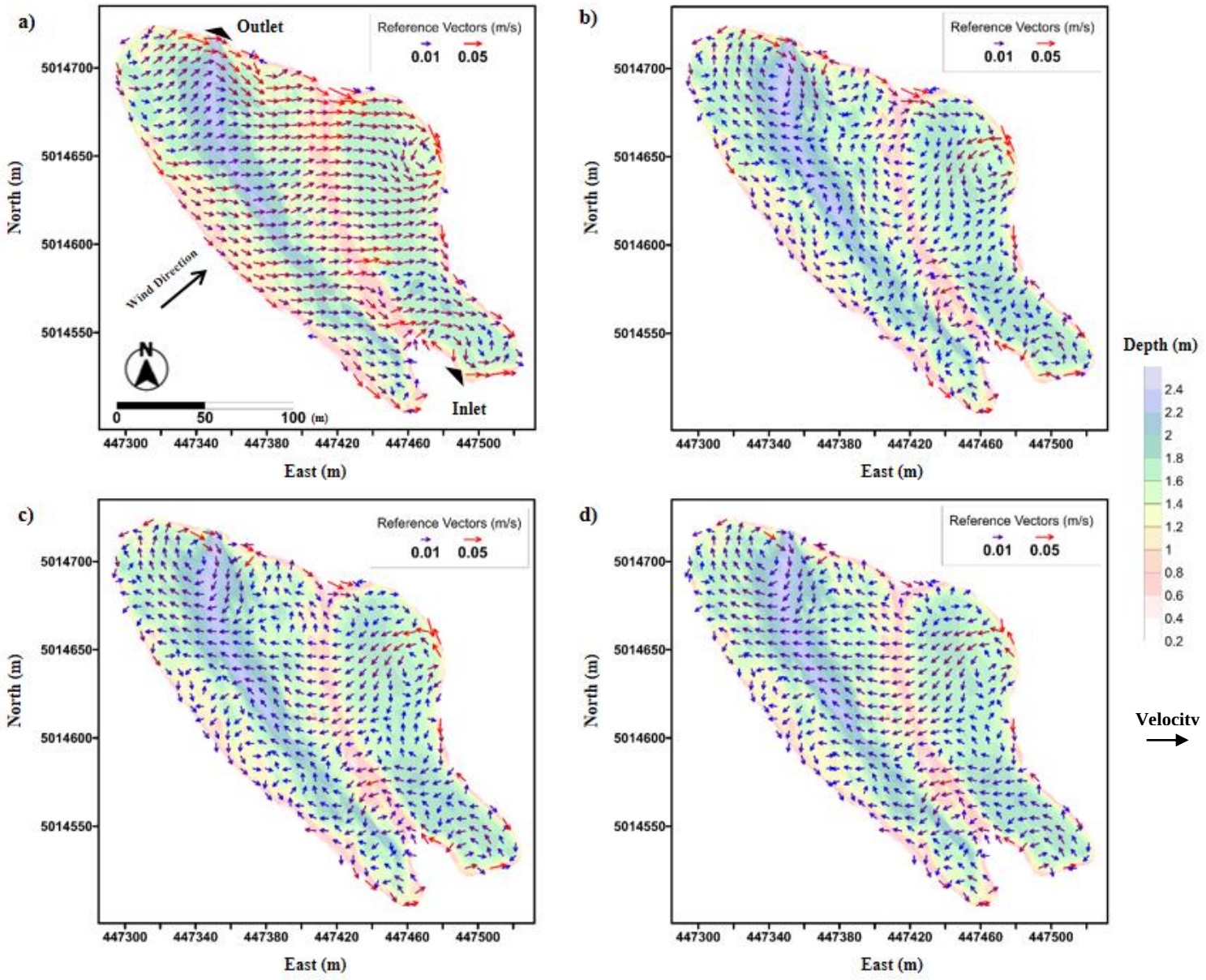

Figure 5.7 Simulated velocity results at RSPII on August 25th, 2015 using MIKE 3 at layers of a) 10 (surface), b) 7, c) 4 and d) 1 (bottom)

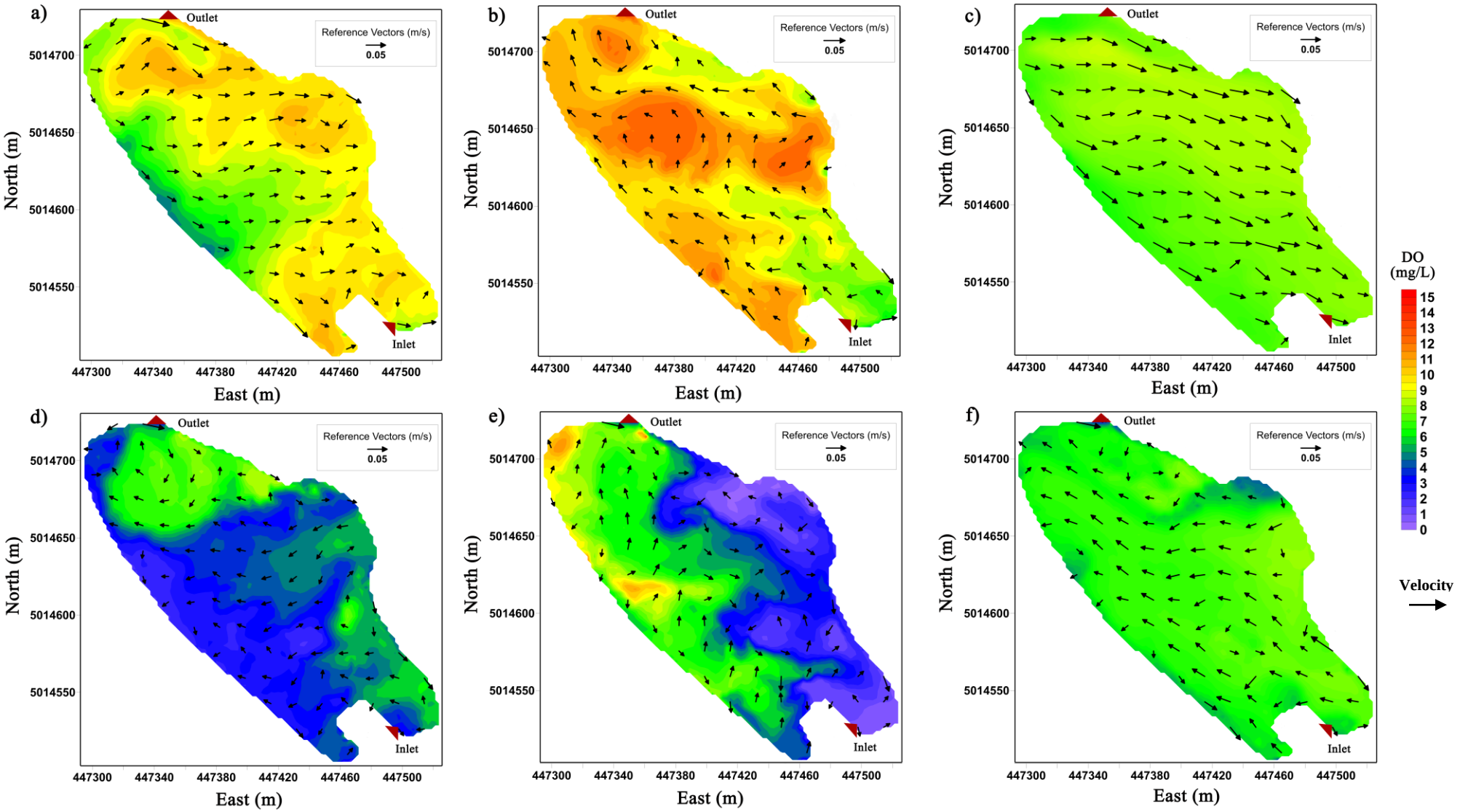

Figure 5.8 Simulated velocity and DO results on August 25th, 2015 (a & d), one low-wind day (b & e), and one high-wind day (c & f) at surface layer 10 (a, b & c) and bottom layer 1 (d, e & f)

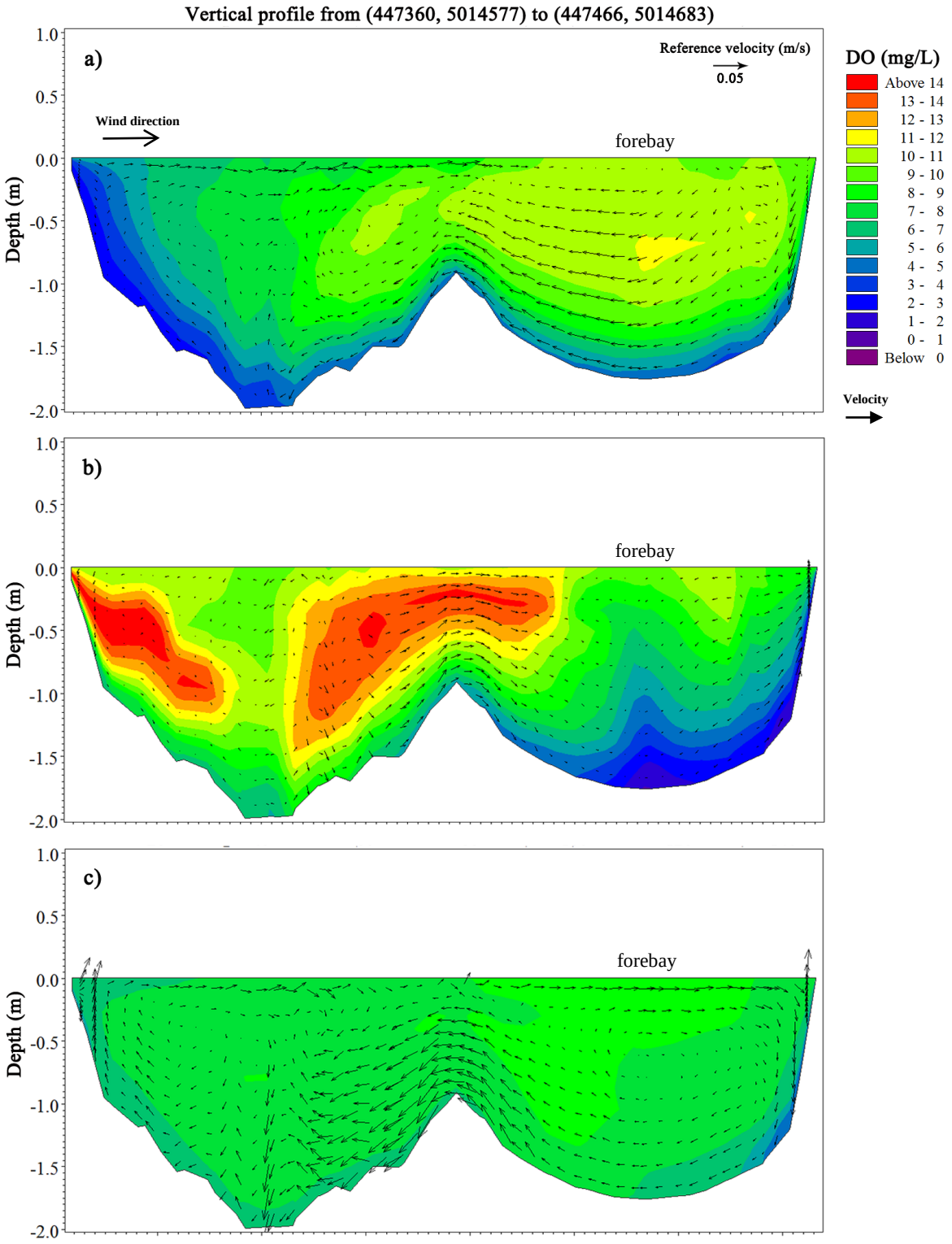

Figure 5.9 Vertical profiles DO concentrations with simulated cross-section velocities on a) August 25th, 2015, b) one low-wind day, and c) one high-wind day

5.5 Conclusion

A three-dimensional MIKE 3 model was carried out to investigate the characteristics of wind-induced hydraulics and its impact on DO concentrations in a shallow SWP (maximum depth < 2.5 m). Validation of the hydrodynamic model was challenging due to the constraint of very small velocity magnitudes within the domain. Despite minimal currents, bottom-mounted aDcp measurements provided current speed and directions within the water column, which allowed for convincing validation of the MIKE 3 wind-driven flow predictions. Spatially distributed SOD and Secchi disk depth are sensitive parameters for DO modelling in small and complex regions according to the current study. The hydrodynamic model suggested a wind dominated circulation was generated even with moderate wind speed, and it also conclusively simulated near-bed countercurrents which were in the opposite direction of the surface wind-generated flow. The DO model results demonstrated that complete mixing can be produced by higher wind speed, due to the fact that low DO water at depth was carried to the surface by upwelling circulation and was possibly replenished during the surface transportation, and then well mixed with the higher DO water. To the contrary, stronger DO stratification was generated with lower wind speed and hypoxic conditions accumulated at depth in the forebay where most of the sedimentation (higher SOD) occurred. The study demonstrated that pond scale mixing first initiated in the downwind water column, and lower DO concentrations can be transported following countercurrent flow at depth. As such, a SWP forebay should be preferrentially placed in the downwind direction to avoid the potential accumulation of hypoxia carried by wind-induced flow.

These results highlighted that wind-driven currents could be important to pond hydraulics within a small shallow water system. Wind-generated circulation was able to cause full mixing with a slightly higher wind speed.

References

Andradóttir, H. Ó. and Mortamet, M-L. (2016). Impact of wind on storm-water pond hydraulics . *J. Hydraul. E.*

Behera, P. K. and Teegavarapu, R. S. V. (2015). Optimization of a stormwater quality management pond system . *Water Resour Manage*, 1083-1095.

Bentzen, T. R., Larsen, T. and Rasmussen, M. R. (2008). Wind effects on retetion time in highway ponds. *Water Sci. Technol*, 1713-1720.

Butts, T. and Evans, R. L. (1979). *Sediment oxygen demand in a shallow oxbow lake.* Urbana: Illinois State Water Survey.

Coman, A. M. and Well, M. G. (2012). Temperature variability in the nearshore benthic boundary layer of Lake Opeongo is due to wind-driven upwelling events. *Can. J. Fish. Aquat. Sci.*, 282-296.

CCN Canadian Climate Normals. (2016, 6 22). Retrieved from Government of Canada: http://climate.weather.gc.ca/climate_normals/index_e.html

Dufresne, C., Duffa, C. and Rey, V. (2014). Wind-forced circulation model and water exchanges through the channel in the Bay of Toulon. *Ocean Dynamics*, 209-224.

Dumas, F., Gendre, R. L., Thomas, Y. and Andréfouët. (2012). Tidal flushing and wind driven circulation of Ahe atoll lagoon (Tuamotu Archipelago, French Polynesia) from in-situ observations and numerical modelling. *Marine Pollution Bulletin*, 425-440.

Fabian, J. and Budinski, L. (2013). Horizontal mixing in the shallow Palic Lake caused by steady and unsteady winds. *Environ. Model. Assess.*, 427-438.

Fan, C. and Wang, W-S. (2008). Influence of biological oxygen demand degradation patterns on water-quality modeling for rivers running through urban areas. *New York Academy of Sciences*, 78-85.

Ferguson, H. L., O'Neill, A. D. J. and Cork, H. F. (1970). Mean evaporation over Canada. *Water resources research*, 1618-1633.

Geemaert, G. L. and Plant W. L. (1990). *Surface waves and fluxes.* The Netherlands: Volume 1-Current theory .

Ghimire, B. K. (2012). *ProQuest Dissertations and Theses "Investigation of Oxygen Half Saturation Coefficients for Nitrification.* Retrieved from http://search.proquest.com.proxy.lib.sfu.ca/docview/918160020?accountid=13800

Glenn, J. S. and Bartell, E. M. (2010). Evaluation short-circuiting potential of stormwater ponds. *World Environmental and Water Resources Congress*, 3942-3951.

Jamu, D. M., Lu, Z. and Piedrahita, R. H. (1999). Relatinship between Secchi disk visibility and chlorophyll a in aquaculture ponds. *Aquaculture*, 205-214.

Jansons, K. and Law, S. (2007). The hydraulic efficiency of simple stormwater ponds. *WSUD (Sydney conference)*.

Jin, K. and Ji, Z. (2004). Case study: modeling of sediment transport and wind-wave impact in Lake Okeechobee. *J Hydraul Eng*, 1055-1067.

Józsa, J. (2014). On the internal boundary layer related wind stress curl and its role in generating shallow lake circulations. *J. Hydrol. Hydromech.*, 16-23.

Kachhwal, L. K., Yanful, E. K. and Rennie, C. D. (2012). A semi-empirical approach for estimation of bed shear stress in a tailings pond. *Environ Earth Sci*, 823-834.

Liang, Q., Borthwick, A. G. L. and Taylor, P. H. (2006). Wind-induced chaotic advection in shallow flow geometries. Part II: Non-circular basins. *J. Hydraul. Res.*, 180-188.

Marsalek, J., Urbonas, B. and Lawrence, I. (2005b). Stormwater management ponds. *Pond Treatment Technology*, 433-459.

Mérette, M. R. (2012). *Primary production and nutrient dynamics of urban ponds.* Ottawa,Ontario, Canada: University of Ottawa, Faculty of Science.

MIKEbyDHI. (2007). *MIKE 21 flow model*. Hørsholm, Denmark: DHI.

MIKEbyDHI. (2012). *MIKE21 &MIKE3 flow model FM. Hydrodynamic and Transport Module. Scientific documentation.* Hørsholm, Denmark: DHI.

MIKEbyDHI. (2016). *ECOlab. Short scientific description.* Hørsholm, Denmark: DHI.

MOE Ministry of the Environment. (2003). *Undertanding Stormwater Management: An Introduction to Stormwater Management Planning and Design.* Government of Ontario.

Pang, C-C., Wang, F-F., Wu, S-Q. and Lai, X-J. (2015). Impact of submerged herbaceous vegetation on wind-induced current in shallow water. *Ecological Engineering*, 387-394.

Pattantyus-Abraham, M., Tel, T., Kramer, T. and Jozsa, J. (2008). Mixing properties of a shallow basin due to wind-induced chaotic flow. *Adv. Water Resour.*, 525-534.

Rennie, C. D. and Villard, P. V. (2004). Site specificity of bed load measurement using an acoustic Doppler current profiler. *Journal of Geophysical Research*, 1-15.

Rodi, W. (1984). *Turbulence models and their applications in hydraulics.* the Netherlands: IAHR, Delft.

Rong, N. and Shan, B. Q. (2016). Total, chemical, and biological oxygen consumption of the sediments in the Ziya River watershed, China. *Environ Sci Pollut Res*, 13438-13447.

Signell, R. P., Beardsley. R. C., Graber, H. C. and Capotondi, A. (1990). Effect of wave-current interaction on wind-driven circulation in narrow, shallow embayments. *Journal of Geophys Resource* , 9671-9678.

Simpson, M.R. (2001), Discharge Measurements Using a Broad-Band Acoustic Doppler Current Profiler, United States Geological Survey Open File Report 01-1, Sacremento, CA.

Sutherland, D. L., Turnbull, M. H. and Craggs, R. J. (2014). Increased pond depth improves algal productivity and nutrient removal in wastewater treatment high rate algal ponds. *Water Research*, 271-281.

Tilzer, M. M. (1988). Secchi disk-chlorophyll relationships in a lake with highly variable phytoplankton biomass. *Hydrobiologia*, 163-171.

Torno, H.C., Marsalek, J. and Desbordes, M. (1985). Urban runoff pollution. *Ecological Sciences* , Series G: vol. 10.

Tu, Y. T., Chiang, P. C., Yang, J., Chen, S. H. and Kao, C. M. (2014). Application of a constructed wetland system for polluted stream remediation. *Journal of Hydrology*, 70-80.

USEPA. (2009). *Stormwater wet pond and wetland management guidebook.* Ellicott City: United States Environmental Protection Agency.

USEPA. (2004). *Stormwater best management practice design guide - volume 3 basin best management practices.* Cincinnati: U. S. Environmental Protection Agency.

Wang, W. C. (1980). Fractionation of sediment oxygen demand. *Water Research* , 603-612.

Wium-Andersen, T., Nielsen, A. H., Hvitved-Jacobsen, T., Brix, H., Arias, C. A. and Vollertsen, J. (2013). Modeling the eutrophication of two mature planted stormwaterponds for runoff control. *Ecological Engineering*, 601-613.

Wium-Andersen, T., Nielsen, A.H., Hvitved-Jacobsen, T. and Vollertsen, J. (2012). Modeling nutrient and pollutant removal in three wet detention ponds. *Urban Environment: Alliance for Global Sustainability Series*, vol. 19.

Wu, J. (1980). Wind-stree coefficients over sea surface and near neutral conditions - a revisit. *Journal of Physical Oceanography*, 727-740.

Wu, J. and Tsanis, I. K. (1994). Numerical study of wind induced water currents. *Journal of Hydraul Eng*, 388-395.

Zounemat-Kermani, M., Scholz, M. and Tondar, M-M. (2015). Hydrodynamic modelling of free water-surface constructed storm water wetlands using a finite volume technique. *Environmental Technology*, 2532-2547.

Chapter 6

Conclusions and Recommendations

The study investigated and discussed dissolved oxygen (DO) seasonal characteristics of a stormwater pond (SWP) of subsequent production of H_2S, along with the correlation of DO spatial distribution and stratification with wind conditions. The implementation of sample collection involved both non-ice covered open water and ice covered seasons, and two SWPs, including one problem pond with H_2S emission and one reference pond without any water quality issue. The conduction of wind impact on DO characteristics was performed at the issue pond.

It is confirmed that H_2S was produced during days with less precipitation in summer and ice covered conditions in winter, with hypoxia performed in proximity to the bottom of the SWP. During non-ice covered months, hypoxia was confined to depth and pond-scale hypoxic conditions were only observed during the period of ice cover. Depth was identified as one of the key factors of hypoxia promotion. No significant correlation of Chl-α and DO or sBOD and DO in the study were observed likely due to the complexity of natural environment. High concentrations of Chl-α was observed in fully ice covered conditions, and the dominant species of blooming algae were also successfully identified as *synurids*, *tabellaria*, and *asterionella*.

A three-dimensional model was successfully conducted to simulate wind-induced flow and its influence on DO characteristics using MIKE 3 (DHI software). The hydrodynamic model successfully simulated near-bed countercurrents in the opposite directions with the surface wind-generated flow, which suggested a wind dominated circulation can be generated even with moderate wind speed. Sediment oxygen demand (SOD) and Secchi depth turned out to be the essential parameters for DO horizontal and vertical distribution in MIKE 3 water quality model. Complete

mixing can be produced by higher wind speed due to the upwelling circulations generated by wind shear. The upwelling circulations carried low DO water at depth, which got replenished during the upwelling process and mixed with the surface water. With lower wind conditions, stronger DO stratification was generated with smaller wind speed and hypoxic conditions accumulated at depth in the forebay where higher SOD occurred. Hence, due to the essential impact of wind-driven currents on pond hydraulics and DO conditions, the wind should be taken into consideration for shallow SWPs design.

Appendix

MIKE 3 ECOlab Module Spatial differentiated Constants Implementation

In this study, spatial distributed Seccih depth and sediment oxygen demand (SOD) were created and implemented. The generation process is illustrated and explained as follows:

Step 1

Mesh Generator (mdf.) was acquired to create and output .mesh file, and expected values of Seccih depth and SOD were manually added within the existed pond shape using scatter point function. However, it needs to be highlighted that since Mesh Generator is designed for bathymetry, it reads points taking consideration of the water surface level, which is 0 m in this case. All the numbers with positive values are seen as 'humps' and negative values are interpreted as 'depth'. As such, the input points should be set as negative values to create this 'fake pond' so that in the next step, 'water' can be filled into the pond and positive 'water depth' can be produced.

Example 1: SOD .mesh file created with scatter data using Mesh Generator (.mdf).

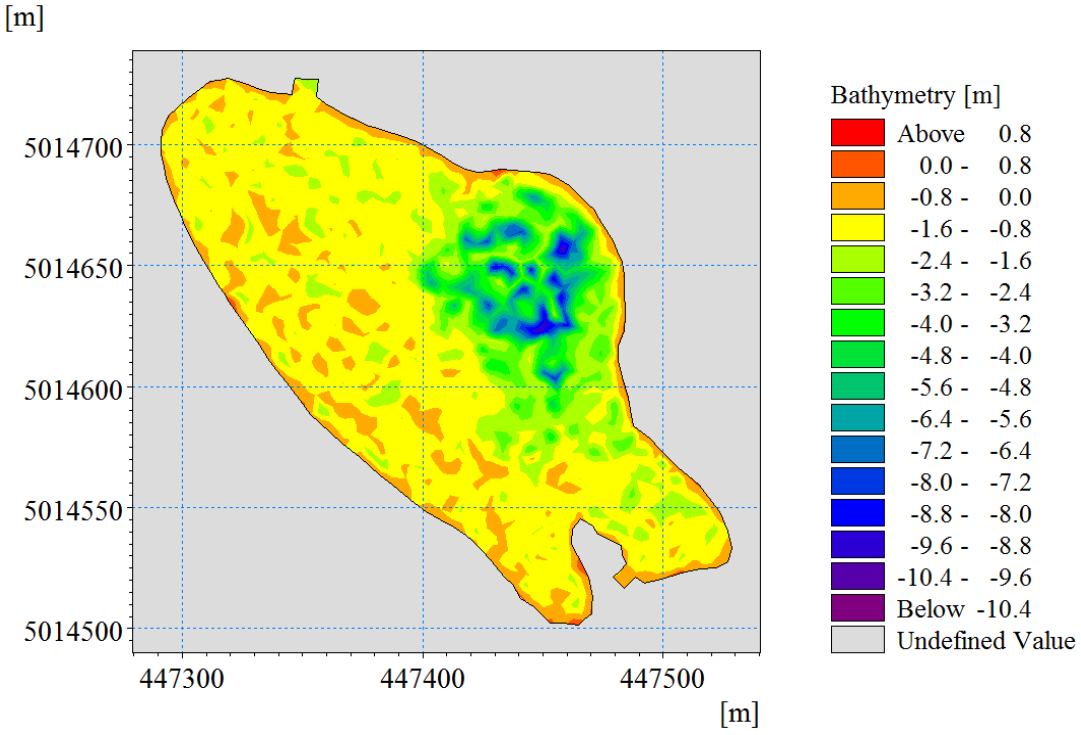

Step 2

To create .dfsu file which is the format requirement for spatial differentiated constants input, MIKE 3 Flow Model FM was needed to generate those values as 'water depth' so that positive values can be read and used for further simulation in the ECOlab module in the study.

Example 2: Seccih depth .dfsu file was created using MIKE 3 Flow Model

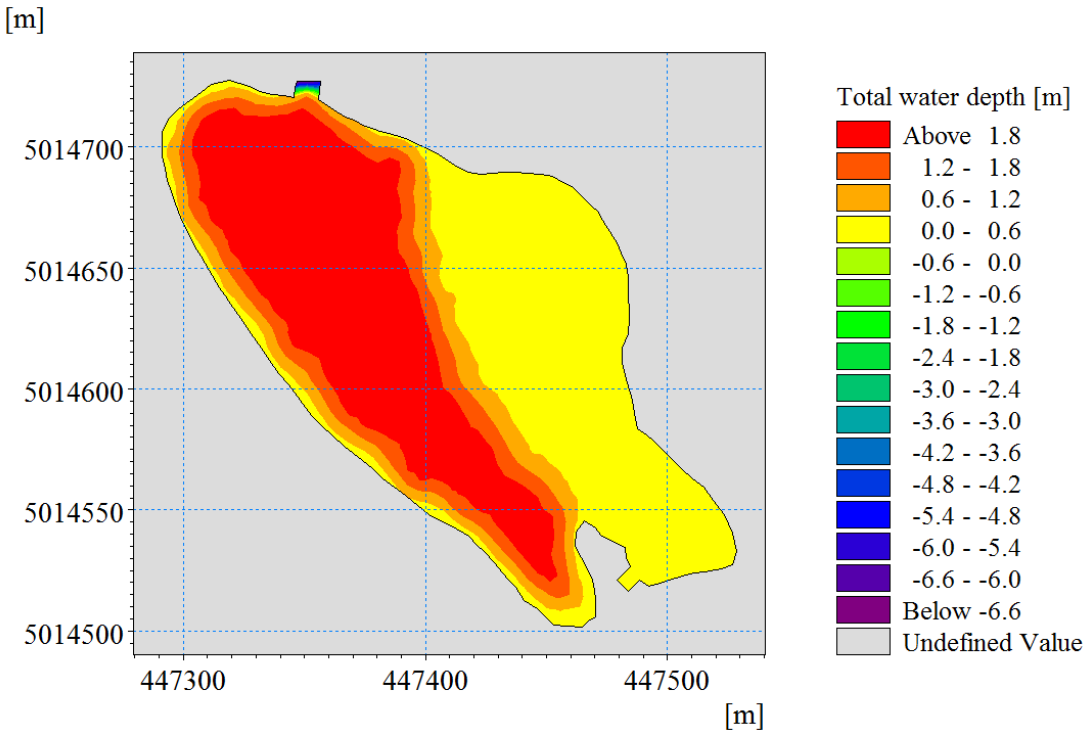

Step 3

In the ECOlab module which spatial distributed constants are required, choose 2D type within the Constants section, and select the .dfsu file for Seccih depth or SOD.